ACS Chemical Neuroscience
Cite This: ACS Chem. Neurosci. 2019, 10, 438−450
Research Article
pubs.acs.org/chemneuro

# Mapping the Orthosteric Binding Site of the Human 5-HT$_3$ Receptor Using Photo-cross-linking Antagonists

Thomas Jack,[†] Michele Leuenberger,[†,∥] Marc-David Ruepp,[†,▽] Sanjeev Kumar V. Vernekar,[#,⊥] Andrew J. Thompson,[‡] Sophie Braga-Lagache,[§] Manfred Heller,[§] and Martin Lochner*[,†,∥]

[†]Department of Chemistry and Biochemistry, University of Bern, Freiestrasse 3, 3012 Bern, Switzerland
[#]Department of Chemistry, University of Warwick, Coventry CV4 7AL, U.K.
[‡]Department of Pharmacology, University of Cambridge, Tennis Court Road, Cambridge CB2 1PD, U.K.
[§]Department of BioMedical Research, Mass Spectrometry and Proteomics Laboratory, University of Bern, Inselspital, 3010 Bern, Switzerland
[∥]Institute of Biochemistry and Molecular Medicine, University of Bern, Bühlstrasse 28, 3012 Bern, Switzerland

Supporting Information

**ABSTRACT:** The serotonin-gated 5-HT$_3$ receptor is a ligand-gated ion channel. Its location at the synapse in the central and peripheral nervous system has rendered it a prime pharmacological target, for example, for antiemetic drugs that bind with high affinity to the neurotransmitter binding site and prevent the opening of the channel. Advances in structural biology techniques have led to a surge of disclosed three-dimensional receptor structures; however, solving ligand-bound high-resolution 5-HT$_3$ receptor structures has not been achieved to date. Ligand binding poses in the orthosteric binding site have been largely predicted from mutagenesis and docking studies. We report the synthesis of a series of photo-cross-linking compounds whose structures are based on the clinically used antiemetic drug granisetron (Kytril). These displaced [$^3$H]granisetron from the orthosteric binding site with low nanomolar affinities and showed specific photo-cross-linking with the human 5-HT$_3$ receptor. Detailed analysis by protein-MS/MS identified a residue (Met-228) near the tip of binding loop C as the covalent modification site.

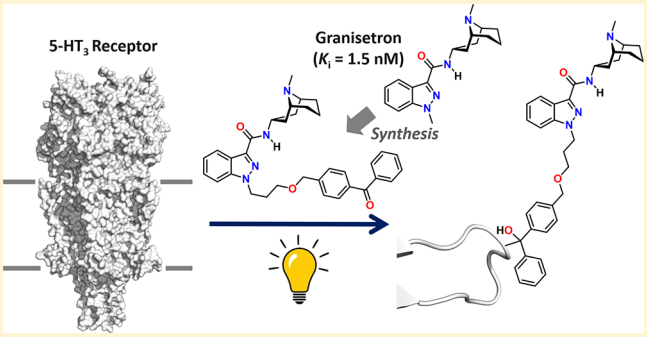


**KEYWORDS:** *5-HT$_3$ receptor, antagonist, granisetron, photo-cross-linking probe, orthosteric binding site, mass spectrometry, docking*



## INTRODUCTION

The serotoninergic system is involved in the control and regulation of many physiological processes such as sleep, appetite, vasoconstriction, body temperature, gastrointestinal motility, and mood. With respect to the latter, an imbalanced function of the serotoninergic system has been strongly associated with depression and mood disorders. Several drugs on the market (e.g., selective serotonin reuptake inhibitors, SSRIs) aim to improve this imbalance, albeit with varying success. Serotonin (5-hydroxytryptamine, 5-HT) is a neurotransmitter that exerts its effect by activating at least 14 different receptors. The large majority of these are metabotropic (5-HT$_{1,2,4-7}$), while only the 5-HT$_3$ receptor is ionotropic and responsible for the fast depolarization of neurons.[1−3] As such, the 5-HT$_3$ receptor shares more structural similarities with other members of the Cys-loop ligand-gated ion channel family that also includes nicotinic acetylcholine (nACh), γ-aminobutyric acid (GABA$_{A/C}$), and glycine receptors. These ion channels consist of five subunits that are pseudosymmetrically assembled around a central ion conducting pore. Each of the five protomers features three structurally distinct domains (Figure 1a): the extracellular domain (ECD), the transmembrane domain (TMD), and the intracellular domain (ICD). The serotonin binding sites (i.e., orthosteric sites) are located in the ECD at the interface of two adjacent protomers formed by the convergence of three peptide loops from one protomer (the principal face, loops A−C) and three loops from the neighboring protomer (the complementary face, loops D−F, Figure 1c).[4]

A class of high-affinity antagonists (the "setrons") that compete with serotonin for the orthosteric 5-HT$_3$ receptor binding sites has been established as antiemetic drugs in the clinic, alleviating the symptoms of nausea and vomiting resulting from chemo- and radiotherapy and general anesthesia.[3] Pharmacological antagonism of 5-HT$_3$ receptors is also used to treat irritable bowel syndrome (IBS). Recent reports indicate, however, that partial 5-HT$_3$ receptor agonism might be a better approach to treat certain types of IBS, as a large group of patients suffer from significant side effects during the current antagonist

**Received:** July 2, 2018
**Accepted:** August 27, 2018
**Published:** August 27, 2018




DOI: 10.1021/acschemneuro.8b00327
ACS Chem. Neurosci. 2019, 10, 438−450

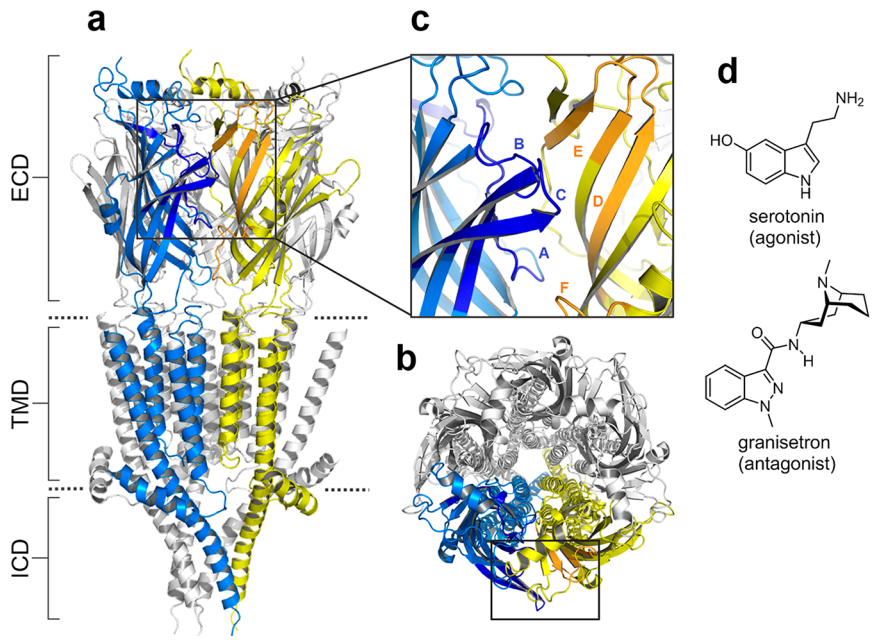


**Figure 1.** (a) View parallel to the plasma membrane of the mouse 5-HT$_3$A receptor (PDB ID 4PIR) with the extracellular (ECD), transmembrane (TMD), and intracellular (ICD) domains indicated. The stabilizing nanobodies have been omitted for clarity. The approximate location of the lipid bilayer is shown by horizontal dotted lines. Two adjacent protomers forming one orthosteric binding site (black box) are highlighted. (b) Extracellular view perpendicular to the plasma membrane of the receptor with one orthosteric binding site (black box) indicated. (c) Close up view of one orthosteric binding site showing the principal face (blue, loops A−C) and complementary face (yellow, loops D−F). (d) Chemical structures of endogenous agonist serotonin and prototypical competitive antagonist granisetron (Kytril).

treatment.[5] Other disorders where 5-HT$_3$ receptors might be involved include depression, drug abuse, schizophrenia, fibromyalgia, pruritus, bulimia nervosa, and pain.[6−8]

Detailed structural information about the 5-HT$_3$ receptor binding sites would be very beneficial for the development of novel compounds to improve current therapies and establish new therapies in other disease areas. A wealth of mutagenesis studies in the past three decades have probed putative binding site residues that often have been deduced from a combination of homology modeling and docking.[9−11] These and other studies have identified residues that are important for ligand binding or channel gating, although extracting detailed noncovalent interactions between functional groups of the ligand and receptor residues is very challenging. Four years ago, the first crystal structure of a mammalian 5-HT$_3$ receptor was presented (Figure 1).[12] The truncated form of the homomeric mouse 5-HT$_3$A receptor was stabilized with nanobodies, and its structure was solved to a resolution of 3.5 Å (PDB ID 4PIR). In this apo structure, the recognition loops of the nanobodies reach into the orthosteric binding site. More recently, the cryo-EM structure of the full length mouse apo-5-HT$_3$A receptor at 4.3 Å resolution was published (PDB ID 6BE1).[13] In a different approach, pentameric acetylcholine binding protein (AChBP), which is homologous to the ECD, was engineered to bind agonists and antagonists with affinities comparable to the 5-HT$_3$ receptor (termed 5HTBP). One such construct was cocrystallized with competitive antagonist granisetron (PDB ID 2YME)[14] and with picomolar-affinity antagonist palonosetron (PDB ID 5LXB),[15] and the complexes were solved to high resolution (2.4 and 2.3 Å, respectively). These models have revealed very detailed noncovalent interactions, such as hydrogen bonds and hydrophobic, $\pi-\pi$, and cation$-\pi$ interactions, between the ligands and binding site residues. Nevertheless, one has to exercise caution when using these binding site models to predict binding orientations of structurally similar ligands at the receptor.[16]

Using photo-cross-linking probes is a well-established technique to capture weak noncovalent interactions between a small molecule and its target protein. In the Cys-loop receptor family, orthosteric and allosteric binding sites on nACh and GABA receptors have been investigated by utilizing photo-cross-linking probes derived from general anesthetics, insecticides, and other modulators in conjunction with protein sequence analysis after labeling (e.g., MS).[17−24] Moreover, covalent labeling can also be utilized to map the binding site(s) of a ligand or to identify the cellular target(s) if unknown. Photo-cross-linking moieties such as diazirines, benzophenones, and phenylazides that are appended to a tolerant position of the bioactive molecule are most commonly employed.[25,26] The photo-cross-linking methodology is applicable to native, wild-type proteins, and if the design of the probe is chosen appropriately (e.g., by using a modifiable linker or additional bioorthogonal functional groups), the target protein can be functionalized further with new properties by way of post-photoaffinity modification (P-PALM).[27,28] However, only a few photo-cross-linking studies have been conducted with 5-HT$_3$ receptors. For instance, Blanton and co-workers have employed the lipophilic, well-known photolabel [$^{125}$I]TID (3-trifluoromethyl-3-(*m*-[$^{125}$I]iodophenyl)-diazirine) to covalently modify receptor residues at the lipid−protein interface.[29] Earlier studies by Lummis and Baker have also shown that intrinsically photoreactive antipsychotic phenothiazines label the 5-HT$_3$ receptor orthosteric binding site; however, a detailed postlabeling sequence analysis was not performed.[30] Therefore, detailed structural information from photolabeling could be beneficial for understanding the binding of ligands at these receptors.

We have previously developed fluorescent[31−33] and PET[34] 5-HT$_3$ receptor ligands derived from the high-affinity competitive



DOI: 10.1021/acschemneuro.8b00327
*ACS Chem. Neurosci.* 2019, 10, 438−450

**Scheme 1. Synthesis of Granisetron-Based Photo-cross-linking Probes**[a]

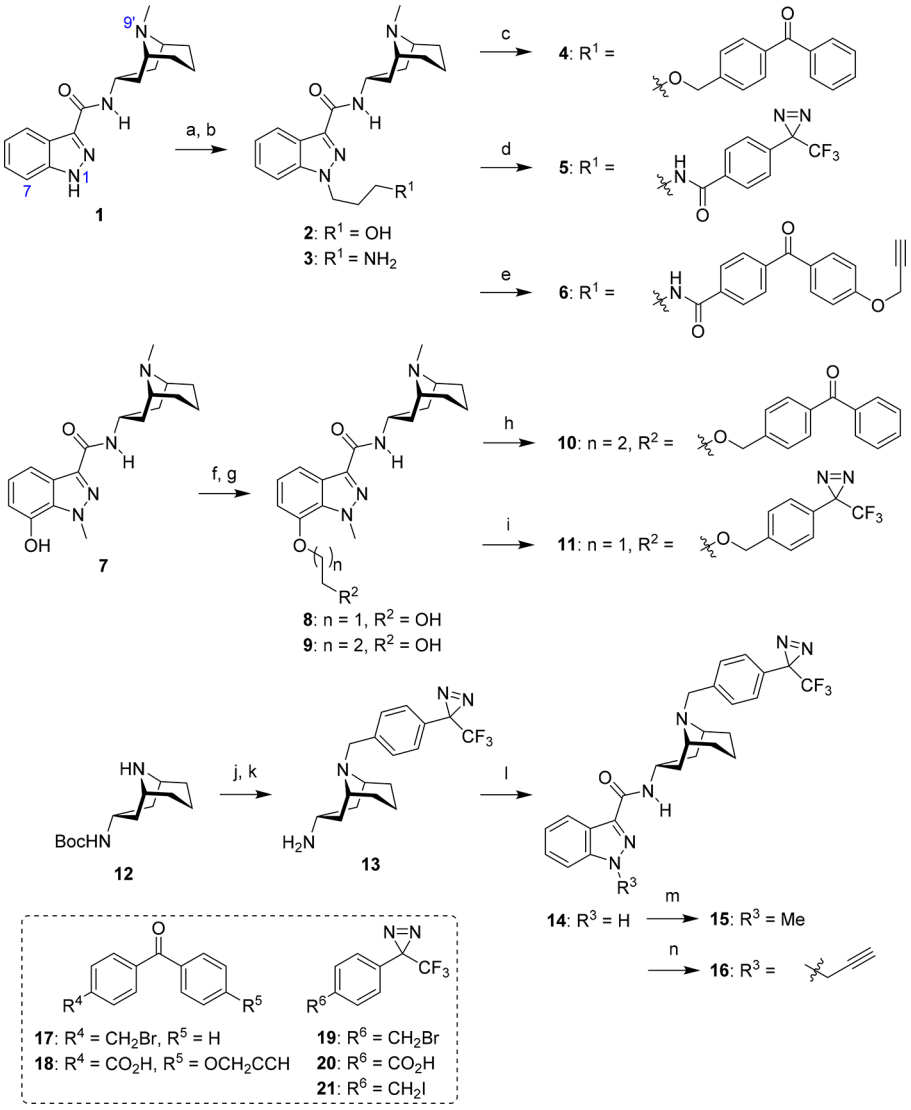


[a]Reagents and conditions: (a) KO$^t$Bu, THF/DMF 5:1, 0 °C; either Br$(CH_2)_3$OTBS or Br$(CH_2)_3$NHBoc, rt, 68% ($R^1$ = OTBS), 78% ($R^1$ = NHBoc); (b) for $R^1$ = OTBS, TBAF, THF, rt, 86% **2**; for $R^1$ = NHBoc, 1.2 M HCl in MeOH, rt, 98% **3**; (c) **2**, NaH, THF/DMF 5:1, 0 °C; **17**, rt, 27%; (d) **3**, **20**, $Et_3N$, HATU, DMF/DCM 3:2, rt, 24%; (e) **18**, $SOCl_2$, MeCN, 80 °C; **3**, DCM, 0 °C to rt, 11%; (f) KO$^t$Bu, THF/DMF 5:1, 0 °C; either Br$(CH_2)_2$OTBS or Br$(CH_2)_3$OTBS, rt, 78% ($n$ = 1), 34% ($n$ = 2); (g) TBAF, THF, rt, 51% **8** ($n$ = 1), 85% **9** ($n$ = 2); (h) **9**, NaH, THF/DMF 5:1, 0 °C; **17**, rt, 20%; (i) **8**, NaH, THF/DMF 5:1, 0 °C; **19**, rt, 35%; (j) $K_2CO_3$, **21**, EtOH, 55 °C, 82%; (k) TFA, DCM, rt, quant; (l) 1*H*-indazole-3-carboxylic acid, DCC, HOBt, DCM/DMF 3:2, rt; **13**, 66%; (m) **14**, KO$^t$Bu, THF/DMF 4:1, 0 °C; MeI, rt, 88%; (n) **14**, $Cs_2CO_3$, DMF, rt; 3-bromoprop-1-yne, 93%. See structure **1** for the numbering of the granisetron core.

antagonist granisetron (Kytril, Figure 1d) and used these probes to study these receptors in cells and live animals. Here we extend these studies of biophysical probes by synthesizing a series of photo-cross-linking probes that were created by appending various photoreactive moieties to three different positions of the granisetron core. Furthermore, we use these probes to specifically photolabel residues in the orthosteric binding site of the 5-$HT_3$ receptor.

## RESULTS AND DISCUSSION

**Design and Synthesis of 5-$HT_3$ Receptor Photo-cross-linking Probes.** Following our previous SAR study of granisetron[35] and design of fluorescent granisetron probes,[31,32] we chose to link the photolabeling moieties to the indazole *N*-1 or C-7 or granatane *N*-9′ position of the antagonist core (Scheme 1). Briefly, either 1*H*-indazole amide **1**[35] or 7-hydroxyindazole amide **7**[31,35] was alkylated with protected linkers, followed by deprotection and subsequent alkylation with benzophenone bromide **17**[36] or diazirine benzyl bromide **19**[37] or amidation with diazirine benzoic acid **20**.[38,39] For accessing the *N*-9′ modified probes **15** and **16**, Boc-protected granatane amine **12**[40] was alkylated first with diazirine benzyl iodide **21**,[41,42] deprotected, coupled to 1*H*-indazole-3-carboxylic acid, and finally *N*-1 alkylated.

We have also synthesized two granisetron probes, **6** and **16**, that, in addition to the photolabeling moieties, contain an alkyne handle to aid post-photoaffinity identification of modified receptors by means of Cu(I)-catalyzed alkyne−azide cycloaddition (CuAAC) reactions. Granisetron probe **6** was obtained through amidation of precursor **3**[35] with benzophenone acid **18**,[43,44] and **16** was synthesized by *N*-1 propargylation of indazole amide **14**.



DOI: 10.1021/acschemneuro.8b00327
ACS Chem. Neurosci. 2019, 10, 438−450

**Pharmacological Characterization of 5-HT$_3$ Receptor Photo-cross-linking Probes.** The binding affinities of the granisetron photo-cross-linking probes **4**–**6**, **10**, **11**, **15**, and **16** for the human homopentameric 5-HT$_3$A receptor were assessed by competition with [$^3$H]granisetron. The $K_i$ values are summarized in Table 1.

**Table 1. Binding Affinities of Granisetron Photo-crosslinking Probes at Human 5-HT$_3$A Receptor**

| compound | p$K_i$[a] | $K_i$ (nM) | $n$ |
|---|---|---|---|
| granisetron | | 1.45[b] | 3 |
| **4** | 10.21 ± 0.38 | 0.06 | 4 |
| **5** | 8.26 ± 0.04 | 5.50 | 4 |
| **6** | 7.48 ± 0.16 | 33.1 | 5 |
| **10** | 9.34 ± 0.11 | 0.46 | 4 |
| **11** | 8.22 ± 0.28 | 6.03 | 3 |
| **15** | 5.67 ± 0.14 | 2138 | 7 |
| **16** | 5.99 ± 0.22 | 1023 | 3 |

[a]Data are the mean of $n$ independent experiments ± SEM and determined from competition binding with [$^3$H]granisetron using HEK293 cell membranes stably expressing 5-HT$_3$AR. [b]Reference 45.

All probes except **15** and **16** exhibited a sub-nanomolar to low nanomolar affinity at the orthosteric binding site of the 5-HT$_3$A receptor. This is in line with our previous findings where appendage of bulky fluorescent dyes to the indazole *N*-1 and *C*-7 positions resulted in high-affinity orthosteric ligands (for the numbering of the granisetron core see structure **1**, Scheme 1).[31,32,35] Although **15** and **16** compete with [$^3$H]-granisetron for the same binding site, their affinities are 3 orders of magnitude lower than the parent ligand. Previously we synthesized *N*-9′-benzyl granisetron[35] that similarly had a lower affinity (p$K_i$ = 6.72 ± 0.24, $K_i$ = 191 nM, $n$ = 6)[16] than the parent ligand, and thus it seems that further substitution at the *para*-position of the phenyl ring is less favorable.

**Photo-cross-linking of 5-HT$_3$ Receptor with Granisetron Probes.** Whole cell lysate from HEK293T cells stably expressing human N-terminal FLAG-tagged 5-HT$_3$A receptor[32] was incubated with either **6**, **16**, or nonspecific alkyne benzophenone **22** (Figure 2), irradiated (at 302 nm for 30 min), and subsequently treated with biotin azide **23** (Figure 2) under CuAAC conditions ($CuSO_4$, TBTA, TCEP). Biotinylated proteins were pulled down with streptavidin beads, eluted, and analyzed by Western blot. Whereas clear biotinylated bands could be observed for **6** in the right mass region for the 5-HT$_3$A receptor (calcd 57.4 kDa for one protomer, exact sequence see Figure S3), photo-cross-linking with probe **16** resulted in almost no bands (Figure S1). This could be due to the significantly lower binding affinity of **16** compared to **6** (Table 1) or that differing binding orientations result in different photo-cross-linking and biotin labeling efficacies. Benzophenone **22**, which is lacking the granisetron moiety, did not give significant photo-cross-linking bands, consistent with its lack of competition with [$^3$H]granisetron.

Affinity-purified human FLAG-tagged 5-HT$_3$A receptor reconstituted in $C_{12}E_9$ micelles[32] was incubated with varying concentrations of granisetron probe **6** or benzophenone alkyne **22** (2.5 μM to 2.5 nM), irradiated, and clicked with biotin azide **23**. Clear, concentration-dependent biotinylated bands at around 60 kDa could be observed for **6** but not for nonbinder **22** (Figure 2a,b). While photo-cross-linking with 25 nM **6** still gave a distinct band for biotinylated 5-HT$_3$A receptor (Figure 2b, lane 3), no such band was observed at 2.5 nM **6** (Figure 2b, lane 4), consistent with this being well below its $K_i$ of 33 nM (Table 1). Blocking the receptor orthosteric binding sites with granisetron prior to incubation with **6** and irradiation reduced the formation of biotinylated 5-HT$_3$A receptor bands on the Western blot (Figure 2d, lane 1 vs 2). Similar to our results from whole-cell lysates, benzophenone **22** gave very little nonspecific photo-cross-linking bands in the presence or absence of granisetron (Figure 2d, lanes 3 and 4). The amount of labeling by **6** in the presence of competitor granisetron was comparable to levels of labeling observed by benzophenone alkyne **22** (Figure 2d, lanes 2–4).

The photo-cross-linking of the 5-HT$_3$A receptor by **6** and **22** was also studied in the plasma membrane of live HEK293T cells stably expressing the FLAG-tagged construct. Cell viability was regularly checked by automated counting throughout the irradiation period (25 min at 302 nm and 0 °C) and did not change (Figure S2). After affinity purification of the 5-HT$_3$A receptors using FLAG-beads, they were reacted with biotin azide **23** under CuAAC conditions and analyzed by Western blot (Figures 2e,f). With **6**, a distinct biotinylation band was detected in the mass region for one 5-HT$_3$A receptor protomer (Figure 2e,f, lane 3), while **22** gave very weak biotinylation background signals, consistent with our experiments with purified receptors in micelles (Figure 2f, lane 2).

**Mass Spectrometry Analysis of Photo-cross-linked Sites.** Affinity-purified FLAG-tagged human 5-HT$_3$A receptor[32] was run on a SDS-PAGE gel and stained with Coomassie, and the band at around 57 kDa was excised. Digestion of the excised band with trypsin followed by mass spectrometry analysis of the resulting peptide fragments gave a sequence coverage of 51% (Figure S3) with the hydrophobic transmembrane sequences TM1–TM4 being particularly difficult to ionize and detect. Optimization of the digestion protocols by also utilizing proteinase K, aspartase N, and endoproteinase LysC allowed the identification of 78% of the whole receptor sequence and 91% of the 5-HT$_3$ receptor ECD (Figure S3). This includes almost full sequence coverage of the orthosteric binding loops A–F (Figure 1).

Having established suitable experimental conditions for labeling 5-HT$_3$ receptors, photo-cross-linking was also attempted using probes **4**, **5**, **10**, **11** and **15**. After incubation and irradiation, Coomassie-stained bands of appropriate receptor protomer mass were excised from SDS-PAGE gels and digested using the previously optimized protocols. For **4** and **10**, mass spectrometry revealed the fragment $^{225}$EFSMESSNYYAEMK$^{238}$ (loop C, Figures 1c and S3) had the mass shift that corresponds to the covalent modification with the probes. Further fragmentation of this peptide by MS/MS identified Met-228 as the primary site of cross-link (Figures 3 and S4). In both cases, the peak at $m/z$ 138.13, stemming from the fragmentation of the 9-methyl-9-azabicyclo[3.3.1]nonane (granatane) moiety of **4** and **10** (Figure S5), could be clearly detected (Figure 3b,c, inset). Met-228 is located close to the tip of loop C of the orthosteric binding site (Figures 1c and 4), in line with our experimental evidence that both **4** and **10** compete for the same binding site as [$^3$H]granisetron with high affinity (Table 1).

**Molecular Modeling.** Based upon the experimental findings that **4** and **10** competitively displace [$^3$H]granisetron and cross-link with Met-228 of loop C, we sought a computational approach to predict possible binding orientations of the two probes in the orthosteric 5-HT$_3$ receptor binding site. We used the high-resolution 5HTBP structure (PDB ID 2YME) as docking template as (i) it has been mutated to mimic the human 5-HT$_3$


DOI: 10.1021/acschemneuro.8b00327
ACS Chem. Neurosci. 2019, 10, 438–450

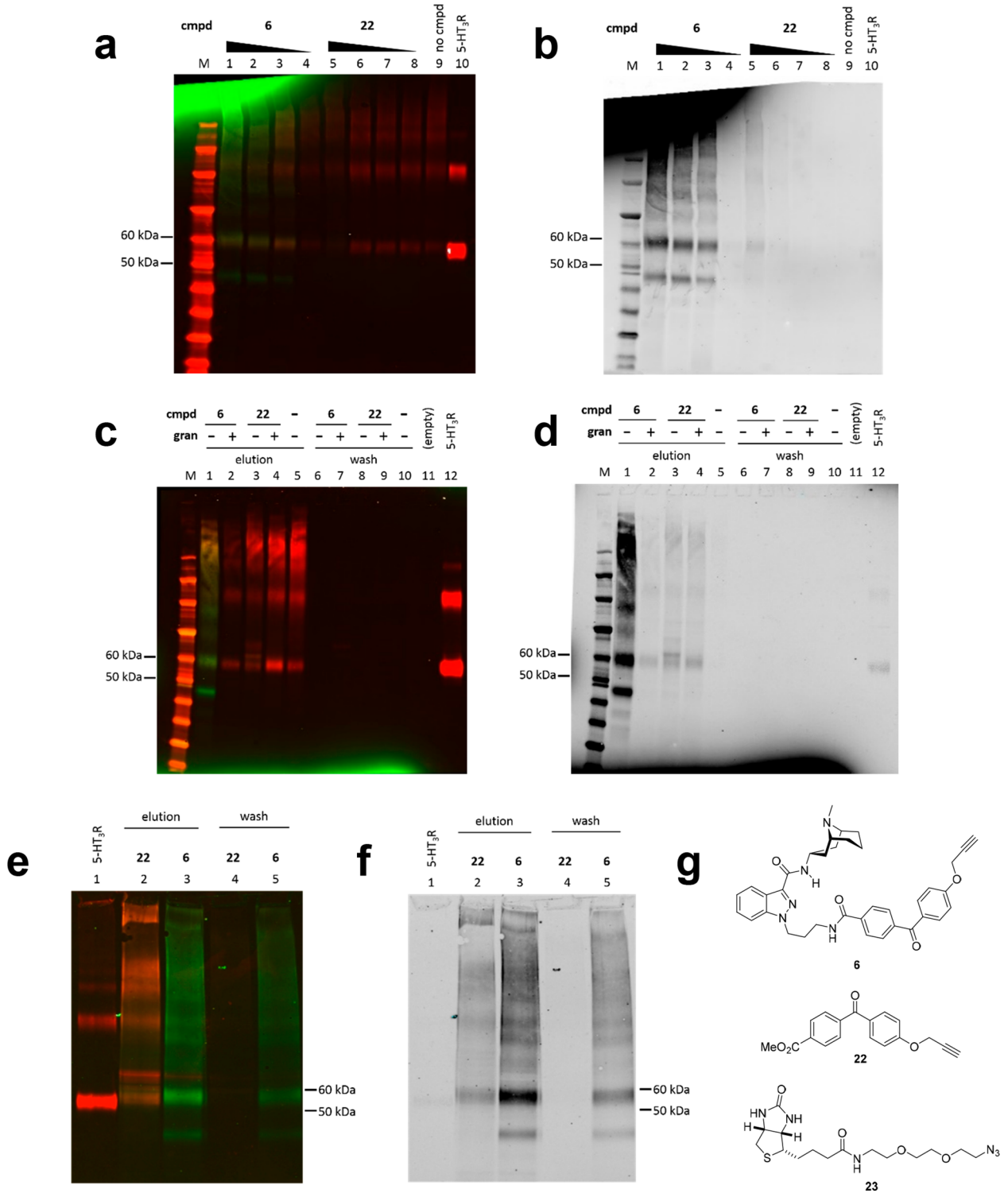


**Figure 2.** Photo-cross-linking of FLAG-tagged h5-$HT_3$A receptor with granisetron probe **6** and control probe **22**. Irradiation of samples was followed by CuAAC reaction with biotin azide **23** and pull down with streptavidin beads. FLAG was visualized with rabbit $\alpha$-FLAG/donkey $\alpha$-rabbit-IRDye 680CW (red), and biotin was visualized with streptavidin-800CW (green) on Western blots. Left panels show overlay of red and green channel detection; right panels are grayscale pictures of green channel (biotin) of the same gel. 5-$HT_3$R, purified, nonirradiated FLAG-tagged h5-$HT_3$A receptor for reference; band between 50 and 60 kDa corresponds to one protomer (ca. 57 kDa); band at higher molecular weight is glycosylated protomer or dimer.[32] Wash indicates supernatant after incubation with streptavidin beads. Elution indicates sample after elution from streptavidin beads. (a, b) Irradiation of purified, micelle-solubilized h5-$HT_3$A receptor in the presence of different concentrations of **6** or **22** (from left to right, 2.5 $\mu$M, 250 nM, 25 nM, 2.5 nM) or no compound. Biotinylated protein band below 50 kDa was not identified. (c, d) Competition of granisetron (gran) with **6** significantly diminishes formation of photo-cross-linked 5-$HT_3$ receptor. (e, f) **6** photo-cross-links 5-$HT_3$ receptor in the plasma membrane of HEK293T cells. (g) Structures of compounds used.



DOI: 10.1021/acschemneuro.8b00327
*ACS Chem. Neurosci.* 2019, 10, 438−450

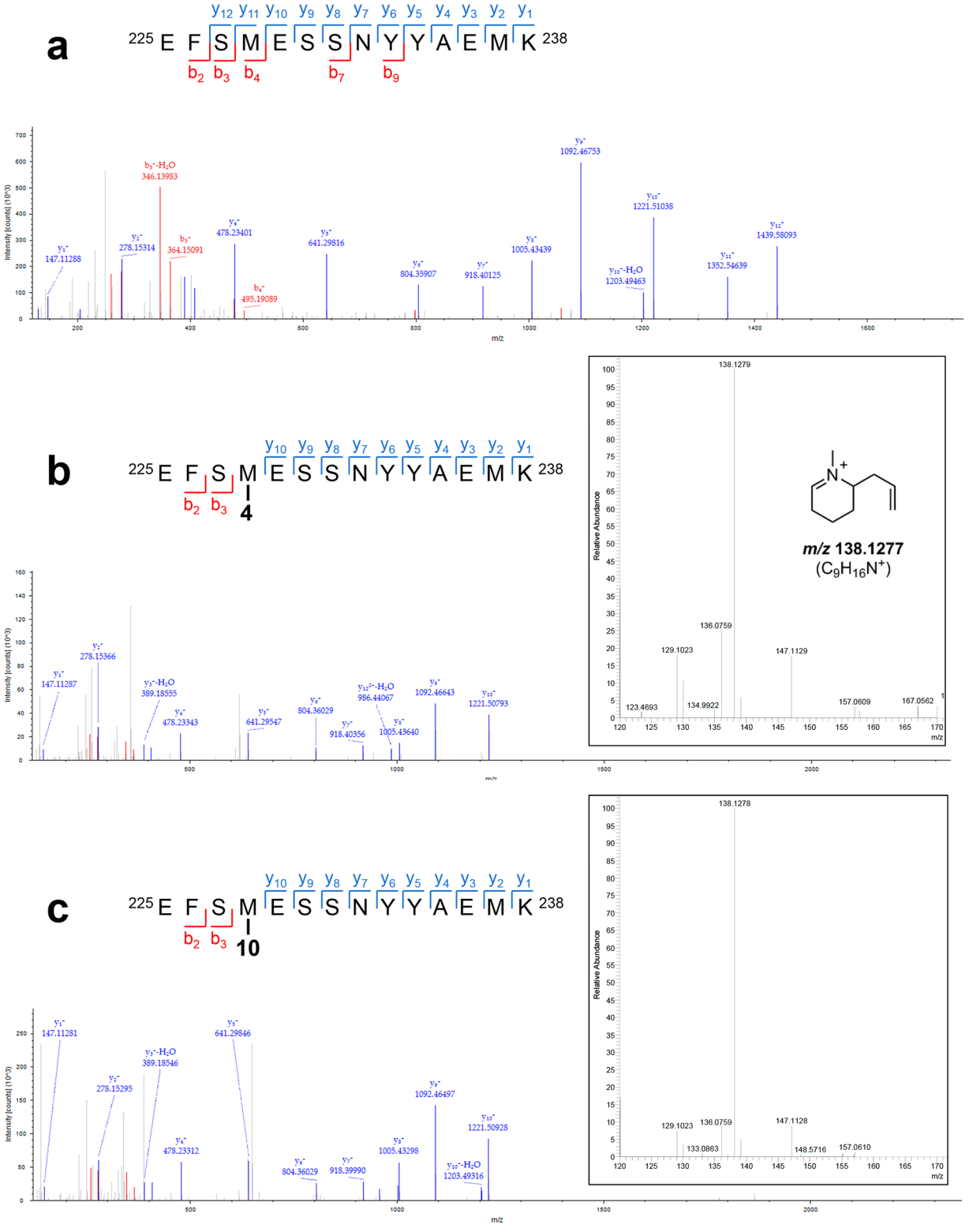


**Figure 3.** Identification of labeling site. Untreated (a) or probe-treated (b, c) human 5-HT$_3$A receptor was digested with LysC/trypsin, the resulting peptides detected by LC-MS/MS and analyzed by Sequest HT (v1.3). Most peaks could be assigned to the y ion series of loop C (Glu-225 to Lys-238). (a) MS/MS spectrum of $m/z$ 858.35 (unmodified peptide $^{225}$EFSMESSNYYAEMK$^{238}$, $z$ = +2). (b) MS/MS spectrum of $m/z$ 756.00 (photo-cross-linked peptide $^{225}$EFSM(**4**)ESSNYYAEMK$^{238}$, $z$ = +3). Inset, Enlarged region of the spectrum showing the diagnostic $C_9H_{16}N^+$ fragment ($m/z$ 138.13) originating from the 9-methyl-9-azabicyclo[3.3.1]nonane (granatane) moiety of the granisetron probes (Figure S5). (c) MS/MS spectrum of $m/z$ 766.00 (photo-cross-linked peptide $^{225}$EFSM(**10**)ESSNYYAEMK$^{238}$, $z$ = +3). Inset, Enlarged region of spectrum. Note how in spectra b and c the y ion series is interrupted at Met-228 by the covalent modification with the probes.

receptor binding site, (ii) the orientation of granisetron in 5HTBP is known to correctly represent the orientation found in the native 5-HT$_3$ receptor,[16] and (iii) it was cocrystallized with granisetron, which is the same recognition moiety of our probes.



DOI: 10.1021/acschemneuro.8b00327
*ACS Chem. Neurosci.* 2019, 10, 438−450

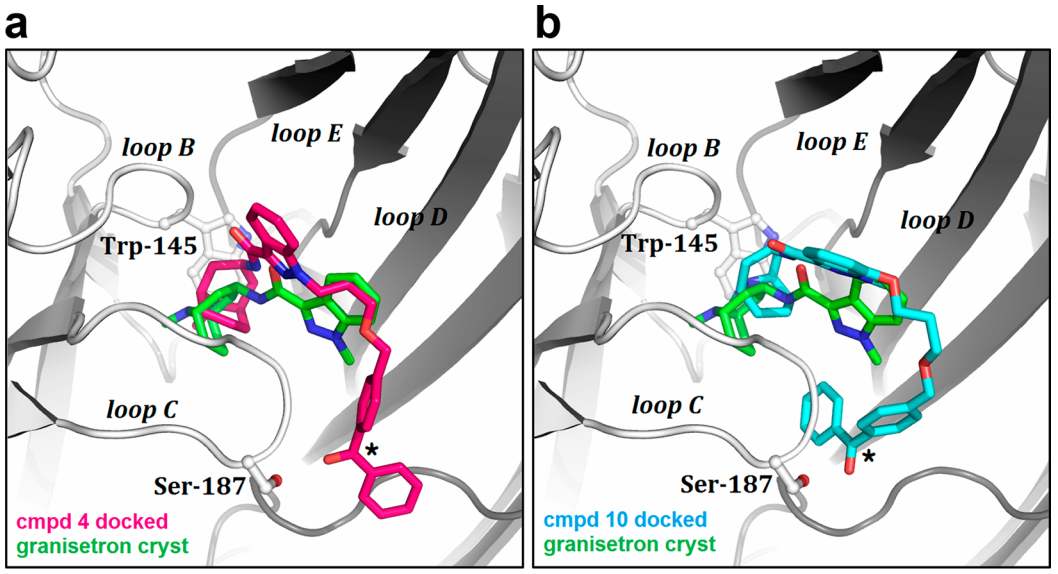


**Figure 4.** Proposed binding orientations of photo-cross-linking probes (a) **4** (deep pink sticks) and (b) **10** (cyan sticks) in the 5HTBP orthosteric binding site. Ligand poses shown are representative of clusters of generated docking solutions (**4**, 3/10; **10**, 2/10 of generated docking solutions) that are the most consistent with evidence from mutagenesis and the pharmacophore model for 5-$HT_3$ receptor ligands.[14,16,47] The peptide chain of the principal face (left) is shown in white and that of the complementary face (right) in gray. Granisetron cocrystallized with 5HTBP (PBD ID 2YME) is shown as reference (green sticks). Side chains of residues Trp-145 and Ser-187 discussed in the text are highlighted as ball-and-sticks. The latter residue aligns with Met-228 of the 5-$HT_3$ receptor (Figure S6b), which was identified as cross-linking site by MS studies (Figure 3). Black asterisk denotes the carbonyl carbon of the benzophenone photo-cross-linking moiety of **4** and **10**. For alternative predicted binding orientations of **4** and **10**, see Figure S7.

For the purpose of validation, granisetron was docked (FRED v2.1) into this binding site model, and its predicted orientation was found to be similar to the binding pose in the crystal structure (Figure S6a). Probes **4** and **10** were also docked into the same site without restraints and resulted in the predicted binding orientations shown in Figures 4 and S7.

In light of experimental evidence, such as mutagenesis and the pharmacophore model for competitive 5-$HT_3$ receptor antagonists, we prefer the orientations shown in Figure 4. For both **4** and **10**, the granisetron moiety is located in the middle of the orthosteric binding site between loops B, C (principal face), D, and E (complementary face). The azabicyclic moiety is pointing toward the centrally located loop B residue Trp-145 (Trp-183 in 5-$HT_3$ receptor, Figure S6b). This highly conserved residue can form cation−$\pi$ interactions with ammonium groups[46,47] and is known to influence the binding of several other orthosteric 5-$HT_3$ receptor ligands.[48] Overall, the granisetron portion of **4** and **10** broadly occupies a similar position and orientation as cocrystallized granisetron in 5HTBP (green sticks, Figure 4). The benzophenone photo-cross-linking group is near the tip of loop C with the carbonyl carbon within short distance of the side chain of Ser-187 that aligns with Met-228 in the 5-$HT_3$ receptor (Figure S6b). The carbonyl group of benzophenones converts into a ketyl radical upon irradiation, which can rapidly react with nearby C−H bonds forming covalent connection.[25] It should be noted that although the orientations in these dock poses are compelling, to confirm the poses requires further experimental validation. Ultimately, probes **4** and **10** are photo-cross-linking conjugates of granisetron, and caution may be needed when predicting binding orientations for other ligands from the poses that are shown.[16]

## CONCLUSIONS

We synthesized nanomolar affinity photo-cross-linking probes that bind to the 5-$HT_3$ receptor orthosteric binding site. Our results demonstrate that the granisetron scaffold is suitable for the attachment of large biophysical tags, in particular at indazole positions *N*-1 and *C*-7. With these probes, we were able to specifically photolabel the receptor at Met-228, which is located near the tip of loop C. Our study also provides design clues for cross-linking probes with cleavable linkers that can be used for post-photoaffinity labeling modifications with reagents such as biotin.[27,28] Here we achieved this in both purified and native receptors providing an opportunity to introduce other biophysical reporters (e.g., small fluorescent dyes) to the tip of the highly mobile binding loop C.

## METHODS

**Chemistry.** For general synthesis methods and synthesis of photo-cross-linking moieties **18**, **20**, **21**, and protected linkers, see the Supporting Information. The synthesis of **1**, **3**, and **7** was described previously.[31,35] Protected granatane **12**[40] and photo-cross-linking moieties **17**[36] and **19**[37] were obtained according to literature procedures, with slight modifications (Supporting Information).

*1-(3-Hydroxypropyl)-N-((1R,3r,5S)-9-methyl-9-azabicyclo[3.3.1]-nonan-3-yl)-1H-indazole-3-carboxamide* (**2**). A suspension of indazole amide **1**[35] (300 mg, 1.01 mmol) in THF/DMF 5:1 (15 mL) was cooled to 0 °C. KO$^t$Bu (124 mg, 1.20 mmol) was added as suspension in dry THF (2 mL), and the mixture was stirred at 0 °C for 15 min. (3-Bromopropoxy)(*tert*-butyl)dimethylsilane (382 mg, 1.51 mmol) was dissolved in dry THF (2 mL) and added to the reaction mixture. Cooling was removed, and the mixture stirred at RT overnight. Solvents were removed *in vacuo*, the residue was taken up in $H_2O$ (10 mL), and the aqueous mixture was extracted with EtOAc (3 × 20 mL). Drying the organic layers over $Na_2SO_4$ and evaporation of the solvent under reduced pressure gave crude TBS-protected indazole (322 mg, 68%) as colorless crystals. $^1$H NMR (300 MHz, $CDCl_3$) $\delta$ 8.39 (d, $J$ = 8.1, 1H), 7.50−7.32 (m, 2H), 6.78 (d, $J$ = 7.6, 1H), 4.66−4.37 (m, 3H), 3.77−3.48 (m, 2H), 3.10 (d, $J$ = 10.1, 2H), 2.64−2.42 (m, 5H), 2.23−2.04 (m, 2H), 1.99 (br, 3H), 1.55−1.50 (m, 1H), 1.44−1.33 (m, 2H), 1.06 (d, $J$ = 9.1, 2H), 0.93 (s, 6H), 0.05 (s, 9H). MS (NSI) $m/z$ 471.31, $[M + H]^+$.

TBS-protected indazole from above (300 mg, 0.64 mmol) and TBAF (335 mg, 1.28 mmol) were dissolved in THF (1.5 mL) and stirred



DOI: 10.1021/acschemneuro.8b00327
*ACS Chem. Neurosci.* 2019, 10, 438−450

overnight at RT. $H_2O$ (8 mL) was added, and the mixture was extracted with DCM (3 × 20 mL). The combined organic layers were washed with $H_2O$ (10 mL), dried over $Na_2SO_4$, and evaporated. After purification with flash chromatography (silica gel, gradient DCM 100% to DCM/MeOH/$Et_3N$ 96:3:1), title compound **2** was obtained as clear oil (196 mg, 86%). $^1H$ NMR (300 MHz, $CDCl_3$) $\delta$ 8.38 (d, $J$ = 8.2, 1H), 7.51−7.38 (m, 2H), 7.30−7.23 (m, 1H), 6.92 (s, 1H), 4.67−4.58 (m, 1H), 4.56 (t, $J$ = 6.7, 2H), 3.63 (t, $J$ = 5.8, 2H), 3.22 (d, $J$ = 12.0, 2H), 2.61 (s, 3H), 2.60−2.50 (m, 2H), 2.25−2.14 (m, 2H), 2.12−1.96 (m, 3H), 1.71−1.54 (m, 3H), 1.30−1.08 (m, 2H). HRMS $m/z$ calcd for $C_{20}H_{29}N_4O_2$ $[M + H]^+$ 357.2285, found 357.2289.

*1-(3-((4-Benzoylbenzyl)oxy)propyl)-N-((1R,3r,5S)-9-methyl-9-azabicyclo[3.3.1]nonan-3-yl)-1H-indazole-3-carboxamide (**4**).* Alcohol **2** (33.4 mg, 93 $\mu$mol) was dissolved in anhydrous THF/DMF 5:1 (6 mL) and cooled to 0 °C. NaH (8.3 mg, 208 $\mu$mol, 60% in oil) was added, and stirring at 0 °C was continued for 5 min. Benzophenone bromide **17** (28.4 mg, 103 $\mu$mol) was added, the cooling was removed, and the suspension was stirred at RT overnight. As reaction control by TLC still showed starting alcohol **2**, more NaH (10.8 mg, 270 $\mu$mol, 60% in oil) and bromide **17** (24 mg, 87 $\mu$mol) were added at RT, and stirring of the red solution was continued at RT overnight. The solvents were removed *in vacuo*, and the residue was purified first by flash chromatography (alumina, DCM) and then by prepTLC (silica gel, DCM/MeOH/$Et_3N$ 96:3:1). To remove traces of $Et_3N$, the product was taken up in little $H_2O$ and extracted with DCM. Drying the DCM layer over $Na_2SO_4$ and evaporation gave **4** (13.9 mg, 27%). UV/vis (PBS buffer): $\lambda_{max}$ abs. 264 nm. IR: 2925, 2850, 1657, 1530, 1309, 1278, 1176, 1104, 924, 733, 704 $cm^{-1}$. $^1H$ NMR (300 MHz, $CDCl_3$) $\delta$ 8.38 (d, $J$ = 8.1, 1H), 7.84−7.76 (m, 4H), 7.64−7.55 (m, 1H), 7.53−7.34 (m, 7H), 7.27 (m, 1H), 6.85 (d, $J$ = 8.1, 1H), 4.66−4.47 (m, 5H), 3.44 (t, $J$ = 5.7, 2H), 3.17 (d, $J$ = 10.5, 2H), 2.63−2.45 (m, 5H), 2.33−2.22 (m, 2H), 2.07−1.93 (m, 3H), 1.63−1.43 (m, 3H), 1.14 (d, $J$ = 9.0 Hz, 2H). $^{13}C$ NMR (75 MHz, $CDCl_3$) $\delta$ 196.5, 162.3, 143.1, 141.4, 137.8, 137.1, 132.6, 130.5, 130.2, 128.5, 127.3, 126.9, 123.2, 122.9, 122.7, 109.3, 77.4, 72.7, 67.2, 51.8, 46.1, 40.8, 40.6, 32.6, 30.1, 25.1, 14.2. HRMS $m/z$ calcd for $C_{34}H_{39}N_4O_3$ $[M + H]^+$ 551.3017, found 551.3011.

*N-((1R,3r,5S)-9-Methyl-9-azabicyclo[3.3.1]nonan-3-yl)-1-(3-(4-(3-(trifluoromethyl)-3H-diazirin-3-yl)benzamido)propyl)-1H-indazole-3-carboxamide (**5**).*[39] Amine **3**[35] (28.4 mg, 66 $\mu$mol) was dissolved in dry DMF/DCM 3:2 (5 mL), and then carboxylic acid **20** (15.3 mg, 66 $\mu$mol), HATU (50.4 mg, 133 $\mu$mol), and three drops of $Et_3N$ were added. The reaction mixture was stirred at RT overnight. Solvents were removed under reduced pressure, and the brown residue was taken up in sat. aq. $NaHCO_3$ (15 mL) and extracted with DCM (3 × 15 mL). The crude oil obtained after evaporation of the organic layers was purified by prepTLC (silica gel, DCM/MeOH/$Et_3N$ 96:3:1). The product still contained some $Et_3N$, which was removed by dissolving in sat. aq. $NaHCO_3$ (2 mL) and extracting with DCM (3 × 2 mL). The DCM layers were dried ($Na_2SO_4$) and evaporated to yield probe **5** (9 mg, 24%) as a slightly yellow oil. UV/vis (PBS buffer): $\lambda_{max}$ abs. 302 nm. IR: 2924, 1650, 1538, 1345, 1310, 1231, 1154, 940, 842, 743 $cm^{-1}$. $^1H$ NMR (300 MHz, $CDCl_3$) $\delta$ 8.10 (d, $J$ = 8.1, 1H), 8.01 (d, $J$ = 8.4, 1H), 7.70 (d, $J$ = 8.4, 2H), 7.41−7.26 (m, 2H), 7.16−7.06 (m, 3H), 6.76−6.68 (m, 1H), 4.82 (s, 1H), 4.34 (t, $J$ = 6.5, 2H), 3.67 (d, $J$ = 9.1, 2H), 3.48−3.35 (m, 2H), 2.86 (s, 3H), 2.62 (t, $J$ = 15.3, 2H), 2.28−2.12 (m, 3H), 2.12−1.86 (m, 4H), 1.51 (d, $J$ = 13.5, 2H), 1.30−1.20 (m, 1H), 0.77 (d, $J$ = 7.5, 2H). $^{13}C$ NMR (75 MHz, CDCl3) $\delta$ 192.2, 166.6, 162.7, 140.8, 137.0, 129.9, 127.5, 127.0, 126.5, 126.1, 122.8, 122.7, 122.2, 109.3, 77.2, 53.5, 46.7, 38.9, 37.6, 30.5, 29.7, 29.0, 24.5, 12.0. HRMS $m/z$ calcd for $C_{29}H_{33}F_3N_7O_2$ $[M + H]^+$ 568.2642, found 568.2621.

*N-((1R,3r,5S)-9-Methyl-9-azabicyclo[3.3.1]nonan-3-yl)-1-(3-(4-(4-(prop-2-yn-1-yloxy)benzoyl)benzamido)propyl)-1H-indazole-3-carboxamide (**6**).* Acid **18** (67 mg, 0.24 mmol) was suspended in MeCN (5 mL), and $SOCl_2$ (128 mg, 1.08 mmol) was added. The mixture was stirred at 80 °C for 3 h and then at RT overnight. Volatiles were removed *in vacuo*, and the brown residue was redissolved in DCM (5 mL) and cooled to 0 °C. A suspension of amine **3**[35] (100 mg, 0.218 mmol) in DCM (2 mL) was added at 0 °C, the cooling was removed, and the reaction mixture was stirred at RT overnight. Solvents were evaporated, and the crude product was purified by flash chromatography (silica gel, DCM/MeOH/$Et_3N$ 96:3:1). Remaining $Et_3N$ after evaporating the appropriate fractions was removed by dissolving in sat. aq. $NaHCO_3$ (2 mL) and extracting with DCM (3 × 2 mL). The DCM layers were dried over $Na_2SO_4$ and evaporated to give probe **6** (15 mg, 11%) as a slightly brown oil. UV/vis (PBS buffer): $\lambda_{max}$ abs. 296 nm. IR: 2927, 2361, 2161, 1653, 1598, 1539, 1282, 1176, 1024, 930 $cm^{-1}$. $^1H$ NMR (300 MHz, $CDCl_3$) $\delta$ 8.28 (d, $J$ = 8.2, 1H), 7.81−7.64 (m, 6H), 7.41−7.28 (m, 2H), 7.26−7.13 (m, 1H), 7.06−6.93 (m, 3H), 6.57 (br, 1H), 4.72 (d, $J$ = 2.4, 2H), 4.64−4.50 (m, 1H), 4.47 (t, $J$ = 6.5, 2H), 3.48 (dd, $J$ = 12.6, 6.4, 3H), 3.16 (d, $J$ = 8.9, 2H), 2.95 (q, $J$ = 7.3, 4H), 2.61−2.37 (m, 6H), 2.34−2.20 (m, 2H), 1.29 (m, 5H). $^{13}C$ NMR (75 MHz, $CDCl_3$) $\delta$ 194.6, 166.7, 161.8, 161.4, 140.8, 138.1, 137.2, 132.5, 130.4, 129.8, 127.2, 126.7, 123.2, 123.0, 122.8, 114.7, 108.9, 77.7, 77.2, 76.3, 55.9, 51.5, 47.0, 46.0, 40.8, 40.4, 37.8, 32.8, 29.1, 24.7, 14.2, 9.7. HRMS $m/z$ calcd for $C_{37}H_{40}N_5O_4$ $[M + H]^+$ 618.3075, found 618.3069.

*7-(2-Hydroxyethoxy)-1-methyl-N-((1R,3r,5S)-9-methyl-9-azabicyclo[3.3.1]nonan-3-yl)-1H-indazole-3-carboxamide (**8**).* Hydroxy indazole **7**[31,35] (133 mg, 0.405 mmol) was dissolved in dry THF/DMF 5:1 (6 mL), and KO$^t$Bu (50 mg, 0.446 mmol) was added. The mixture was cooled to 0 °C and stirred for 30 min. (2-Bromoethoxy)(*tert*-butyl)dimethylsilane (114 mg, 0.477 mmol) dissolved in dry THF (1.5 mL) was added, the cooling was removed, and the reaction mixture was stirred at RT overnight. Reaction control by TLC (silica gel, DCM/MeOH/$Et_3N$ 96:3:1) still indicated the presence of starting material **7**. More KO$^t$Bu (29 mg, 0.258 mmol) and TBS-protected bromide (46 mg, 0.192 mmol) were thus added, and stirring at RT continued for 4 h. Solvents were removed under reduced pressure, and the residue was purified by flash chromatography (alumina, gradient DCM 100% to DCM/MeOH 99:1 and then DCM/MeOH 95:5) giving the TBS-protected alcohol (153 mg, 78%). $^1H$ NMR (300 MHz, $CDCl_3$) $\delta$ 7.91 (d, $J$ = 8.2, 1H), 7.09 (t, $J$ = 7.9, 1H), 6.72 (m, 2H), 4.64−4.42 (m, 1H), 4.32 (s, 3H), 4.18 (t, $J$ = 4.9, 2H), 4.03 (t, $J$ = 4.9, 2H), 3.07 (d, $J$ = 10.4, 2H), 2.59−2.42 (m, 5H), 2.00−1.89 (m, 3H), 1.49 (m, 1H), 1.35 (t, $J$ = 12.4, 2H), 1.04 (d, $J$ = 8.4, 2H), 0.84 (s, 9H), 0.08 (s, 6H). $^{13}C$ NMR (75 MHz, $CDCl_3$) $\delta$ 162.0, 145.4, 137.3, 133.0, 125.2, 123.2, 115.0, 106.7, 69.9, 61.6, 51.3, 40.7, 39.5, 36.4, 33.1, 31.4, 25.8, 24.9, 18.3, 14.3, −5.4. HRMS $m/z$ calcd for $C_{26}H_{43}N_4O_3Si$ $[M + H]^+$ 487.3099, found 487.3091.

To a solution of TBS-protected alcohol from above (153 mg, 0.315 mmol) in THF (5 mL) was added a solution of TBAF (165 mg, 0.631 mmol) in THF (1 mL). The reaction mixture was stirred at RT for 2 d. $H_2O$ (15 mL) and 2 M aq. NaOH (5 mL) were added, and the solution was extracted with DCM (4 × 20 mL). The organic layers were dried ($Na_2SO_4$) and reduced *in vacuo*. Flash chromatography (alumina, gradient DCM 100% to DCM/MeOH 19:1) of the residue gave title alcohol **8** (60 mg, 51%). $^1H$ NMR (300 MHz, $CDCl_3$) $\delta$ 7.80 (d, $J$ = 8.2, 1H), 6.96 (t, $J$ = 7.9, 1H), 6.68 (d, $J$ = 8.4, 1H), 6.56 (d, $J$ = 7.5, 1H), 4.54−4.35 (m, 1H), 4.19 (s, 3H), 4.14−4.07 (m, 2H), 4.01−3.88 (m, 2H), 2.99 (d, $J$ = 10.6, 2H), 2.51−2.34 (m, 5H), 1.89−1.80 (m, 3H), 1.43 (m, 1H), 1.31−1.19 (m, 2H), 0.95 (d, $J$ = 9.8, 2H). One proton was not detected due to rapid exchange. HRMS $m/z$ calcd for $C_{20}H_{29}N_4O_3$ $[M + H]^+$ 373.2234, found 373.2242.

*7-(3-Hydroxypropoxy)-1-methyl-N-((1R,3r,5S)-9-methyl-9-azabicyclo[3.3.1]nonan-3-yl)-1H-indazole-3-carboxamide (**9**).* Compound **9** was synthesized according to the procedure for **8**, using **7**[31,35] (116 mg, 0.353 mmol), KO$^t$Bu (44 mg, 0.392 mmol), and (3-bromopropoxy)(*tert*-butyl)dimethylsilane (107 mg, 0.423 mmol). Aqueous work up with $H_2O$ (10 mL) and DCM (3 × 15 mL) gave the crude product, which was purified by flash chromatography (silica gel, DCM/MeOH/$Et_3N$ 96:3:1). Residual $Et_3N$ in the product was removed by extraction (DCM/$H_2O$) yielding the TBS-protected alcohol (60.7 mg, 34%) as a yellowish solid. $^1H$ NMR (300 MHz, $CDCl_3$) $\delta$ 7.91−7.84 (m, 1H), 7.06 (t, $J$ = 7.9, 1H), 6.74−6.64 (m, 2H), 4.60−4.40 (m, 1H), 4.27 (s, 3H), 4.17 (t, $J$ = 6.1, 2H), 3.81 (t, $J$ = 6.1, 2H), 3.05 (d, $J$ = 10.5, 2H), 2.56−2.39 (m, 5H), 2.05 (p, $J$ = 6.1, 2H), 1.92 (dd, $J$ = 10.6, 3.4, 3H), 1.53−1.41 (m, 1H), 1.41−1.26 (m, 2H), 1.02


DOI: 10.1021/acschemneuro.8b00327
ACS Chem. Neurosci. 2019, 10, 438−450

(d, $J$ = 9.6, 2H), 0.84 (s, 9H), 0.00 (s, 6H). HRMS $m/z$ calcd for $C_{27}H_{45}N_4O_3Si$ $[M + H]^+$ 501.3255, found 501.3256.

Following the procedure for **8**, TBS-deprotection was carried out using protected alcohol from above (60 mg, 0.120 mmol) and TBAF (63 mg, 0.240 mmol). Flash chromatography of the crude product (alumina, gradient DCM 100% to DCM/MeOH 19:1) gave title alcohol **9** (39.5 mg, 85%). $^1$H NMR (300 MHz, $CDCl_3$) $\delta$ 7.82 (d, $J$ = 7.8, 1H), 7.00 (t, $J$ = 7.9, 1H), 6.71−6.57 (m, 2H), 4.53−4.36 (m, 1H), 4.21 (s, 3H), 4.16 (t, $J$ = 6.0, 2H), 3.82 (t, $J$ = 6.1, 2H), 2.99 (d, $J$ = 10.6, 2H), 2.51−2.33 (m, 5H), 2.06 (quin, $J$ = 6.1, 2H), 1.95−1.77 (m, 3H), 1.42 (d, $J$ = 5.5, 1H), 1.34−1.20 (m, 2H), 0.96 (d, $J$ = 9.9, 2H). One proton was not detected due to rapid exchange.

*7-(3-((4-Benzoylbenzyl)oxy)propoxy)-1-methyl-N-((1R,3r,5S)-9-methyl-9-azabicyclo[3.3.1]nonan-3-yl)-1H-indazole-3-carboxamide (**10**).* Alcohol **9** (19.7 mg, 51.1 $\mu$mol) was dissolved in dry THF/DMF 5:1 (3.5 mL) and cooled to 0 °C, and NaH (9 mg, 225 $\mu$mol) was added. After stirring for 5 min at 0 °C bromide **17** (21 mg, 76 $\mu$mol) was added in one portion, the cooling was removed, and the reaction mixture was stirred at RT overnight. The solvents were removed *in vacuo* and the residue purified by prepTLC (silica gel, DCM/MeOH/$Et_3N$ 96:3:1). $Et_3N$ contaminating the product was removed by aqueous extraction (DCM/$H_2O$) and finally gave probe **10** (5.9 mg, 20%) as yellowish solid. IR: 2923, 2855, 2361, 1654, 1532, 1507, 1258, 1113, 735, 701, 631 cm$^{-1}$. $^1$H NMR (300 MHz, $CDCl_3$) $\delta$ 7.92 (d, $J$ = 7.7, 1H), 7.80−7.70 (m, 4H), 7.63−7.55 (m, 1H), 7.52−7.40 (m, 4H), 7.10 (t, $J$ = 7.9, 1H), 6.79−6.70 (m, 2H), 4.62 (s, 2H), 4.60−4.44 (m, 1H), 4.30−4.19 (m, 5H), 3.75 (t, $J$ = 6.1, 2H), 3.11 (d, $J$ = 10.5, 2H), 2.60−2.44 (m, 5H), 2.28−2.16 (m, 2H), 2.02−1.91 (m, 3H), 1.55−1.47 (m, 1H), 1.44−1.32 (m, 2H), 1.07 (d, $J$ = 9.9, 2H). $^{13}$C NMR (75 MHz, $CDCl_3$) $\delta$ 196.3, 162.0, 145.4, 143.0, 137.6, 137.3, 136.9, 132.8, 132.4, 130.3, 130.0, 128.3, 127.1, 125.2, 123.3, 114.9, 106.2, 77.2, 72.5, 67.0, 65.1, 51.4, 40.6, 39.5, 32.9, 29.7, 29.7, 25.0, 14.3. HRMS $m/z$ calcd for $C_{35}H_{41}N_4O_4$ $[M + H]^+$ 581.3122, found 581.3122.

*1-Methyl-N-((1R,3r,5S)-9-methyl-9-azabicyclo[3.3.1]nonan-3-yl)-7-(2-((4-(3-(trifluoromethyl)-3H-diazirin-3-yl)benzyl)oxy)ethoxy)-1H-indazole-3-carboxamide (**11**).* Compound **11** was obtained following the procedure for **10**, using alcohol **8** (30 mg, 80.6 $\mu$mol), NaH (10 mg, 250 $\mu$mol), and diazirine bromide **19** (40 mg, 100 $\mu$mol). The crude product was purified by prepTLC (silica gel, DCM/MeOH/$Et_3N$ 96:3:1), and residual $Et_3N$ was removed from the product by aqueous extraction (DCM/$H_2O$). This yielded probe **11** (16.1 mg, 35%). IR: 2924, 2864, 2358, 2161, 2029, 1977, 1653, 1533, 1258, 1153, 938, 668 cm$^{-1}$. $^1$H NMR (300 MHz, $CDCl_3$) $\delta$ 7.87 (d, $J$ = 7.8, 1H), 7.31 (d, $J$ = 8.5, 2H), 7.11 (d, $J$ = 8.1, 2H), 7.07−6.99 (m, 1H), 6.69 (d, $J$ = 8.4, 1H), 6.64 (d, $J$ = 7.5, 1H), 4.56 (s, 2H), 4.52−4.40 (m, 1H), 4.29−4.16 (m, 5H), 3.89−3.81 (m, 2H), 3.04 (d, $J$ = 10.1, 2H), 2.54−2.37 (m, 5H), 1.96−1.84 (m, 3H), 1.46 (d, J = 5.8, 1H), 1.40−1.23 (m, 2H), 1.00 (d, $J$ = 9.2, 2H). $^{13}$C NMR (75 MHz, $CDCl_3$) $\delta$ 177.1, 162.1, 145.3, 139.9, 137.51, 133.1, 128.8, 128.0, 126.8, 125.4, 123.3, 115.5, 106.8, 77.4, 72.7, 68.9, 67.8, 51.5, 40.8, 39.6, 33.2, 25.1, 14.5. HRMS $m/z$ calcd for $C_{29}H_{34}F_3N_6O_3$ $[M + H]^+$ 571.2639, found 571.2640.

*(1R,3r,5S)-9-(4-(3-(Trifluoromethyl)-3H-diazirin-3-yl)benzyl)-9-azabicyclo[3.3.1]nonan-3-amine (**13**).* Granatane **12**[40] (30 mg, 0.125 mmol) was dissolved in EtOH (4 mL), and $K_2CO_3$ (35 mg, 0.253 mmol) and diazirine iodide **21** (40 mg, 0.098 mmol) were added. The suspension was first stirred at RT overnight and then heated at 55 °C for 3.5 h. The solvent was reduced to about 2 mL *in vacuo*, DCM (10 mL) was added, and the mixture was extracted with $H_2O$. The water phases were washed with DCM (2 × 10 mL). The combined organic layers were dried over $Na_2SO_4$ and evaporated. The crude product was purified by flash chromatography (silica gel, gradient hexanes 100% to hexanes/EtOAc 99:1 to hexanes/EtOAc 7:3), giving the *N*-alkylated granatane (36 mg, 82%). $^1$H NMR (300 MHz, $CDCl_3$) $\delta$ 7.31 (d, $J$ = 6.9, 2H), 7.05 (d, $J$ = 7.3, 2H), 4.22 (s, 1H), 4.01 (s, 1H), 3.73 (s, 2H), 2.95 (d, $J$ = 10.5, 2H), 2.29 (dd, $J$ = 17.9, 12.0, 2H), 1.83 (d, $J$ = 2.9, 3H), 1.39 (s, 9H), 1.22 (s, 1H), 1.08 (t, $J$ = 12.6, 2H), 0.93 (d, $J$ = 10.1, 2H). $^{13}$C NMR (75 MHz, $CDCl_3$) $\delta$ 142.5, 128.6, 127.4, 126.4, 79.1, 77.2, 55.4, 49.4, 33.9, 29.7, 28.5, 24.8, 14.2, 14.1. HRMS $m/z$ calcd for $C_{22}H_{30}F_3N_4O_2$ $[M + H]^+$ 439.2315, found 439.2316.

To a solution of Boc-protected granatane from above (30 mg, 0.068 mmol) in DCM (1 mL) was added TFA (0.25 mL), and the reaction mixture was stirred at RT for 6 h. The volatiles were removed *in vacuo*, and the residue was taken up in DCM (6 mL) and extracted with sat. aq. $NaHCO_3$ (3 mL). The aqueous phase was extracted with DCM (3 × 4 mL), and the combined organic layers were dried over $Na_2SO_4$ and evaporated. This gave title compound **13** (24.5 mg, quant.). $^1$H NMR (300 MHz, $CDCl_3$) $\delta$ 7.29 (d, $J$ = 8.5, 2H), 7.05 (d, $J$ = 8.0, 2H), 3.74 (s, 2H), 3.33−3.16 (m, 1H), 2.92 (d, $J$ = 11.4, 2H), 2.18 (td, $J$ = 11.2, 5.7, 2H), 1.93−1.72 (m, 3H), 1.48−1.38 (m, 1H), 1.12−0.99 (m, 2H), 0.94 (d, $J$ = 12.9, 2H). Two protons (amine) were not observed due to rapid exchange. $^{13}$C NMR (75 MHz, $CDCl_3$) $\delta$ 142.9, 128.5, 127.4, 126.3, 122.2 (q, $J$ = 274.7), 55.4, 49.6, 43.0, 37.3, 29.7, 24.9, 14.2. HRMS $m/z$ calcd for $C_{17}H_{22}F_3N_4$ $[M + H]^+$ 339.1791, found 339.1780.

*N-((1R,3r,5S)-9-(4-(3-(Trifluoromethyl)-3H-diazirin-3-yl)benzyl)-9-azabicyclo[3.3.1]nonan-3-yl)-1H-indazole-3-carboxamide (**14**).* Indazole-3-carboxylic acid (19.4 mg, 0.12 mmol), DCC (27.4 mg, 0.133 mmol), and HOBt (15 mg, 0.111 mmol) were dried in high-vacuum for 20 min and then dissolved under dry conditions in DCM/DMF 3:2 (5 mL). After stirring the solution for 2 h at RT, granatane **13** (22.8 mg, 0.067 mmol) dissolved in DCM (3 mL) was added dropwise, and the reaction mixture was stirred at RT overnight. The solvents were removed under reduced pressure, and the residue was dissolved in DCM (5 mL) and extracted with sat. aq. $NaHCO_3$ (3 mL). The aqueous phase was extracted with DCM (3 × 6 mL), and the combined organic layers were dried ($Na_2SO_4$) and evaporated. The crude product was purified by flash chromatography (silica gel, DCM/MeOH/$Et_3N$ 96:3:1) and prepHPLC (reverse phase, gradient $H_2O$ 100% + 0.1% TFA to $H_2O$/MeCN 4:6 + 0.1% TFA to MeCN 100% + 0.1% TFA, $t_R$ (product) = 28 min). The fractions were lyophilized, and the isolated TFA salt was dissolved in $H_2O$ (1 mL) and extracted into $CHCl_3$ (3 mL). Evaporation of the organic phase gave indazole carboxamide **14** (21.6 mg, 66%). $^1$H NMR (300 MHz, $CDCl_3$) $\delta$ 10.78 (br, 1H), 8.37 (d, $J$ = 8.1, 1H), 7.45 (d, $J$ = 8.4, 1H), 7.40−7.29 (m, 3H), 7.28−7.19 (m, 1H), 7.04 (d, $J$ = 8.0, 2H), 6.83 (d, $J$ = 8.7, 1H), 4.71−4.45 (m, 1H), 3.77 (s, 2H), 3.00 (d, $J$ = 11.1, 2H), 2.41 (td, $J$ = 11.9, 6.2, 2H), 1.94−1.80 (m, 3H), 1.49 (d, $J$ = 9.4, 1H), 1.35−1.21 (m, 2H), 0.97 (d, $J$ = 10.9, 2H). $^{13}$C NMR (75 MHz, $CDCl_3$) $\delta$ 162.3, 157.1, 142.5, 141.5, 139.5, 128.7, 127.5, 127.2, 126.4, 122.7 (d, $J$ = 2.7), 122.2 (q, $J$ = 274.3), 122.0, 109.9, 55.5, 53.4, 49.3 (d, $J$ = 7.7), 41.3, 33.9, 33.5, 28.1, 25.6, 24.9 (d, $J$ = 6.6), 14.2. HRMS $m/z$ calcd for $C_{25}H_{26}F_3N_6O$ $[M + H]^+$ 483.2115, found 483.2100.

*1-Methyl-N-((1R,3r,5S)-9-(4-(3-(trifluoromethyl)-3H-diazirin-3-yl)benzyl)-9-azabicyclo[3.3.1]nonan-3-yl)-1H-indazole-3-carboxamide (**15**).* Indazole carboxamide **14** (16 mg, 0.033 mmol) was dissolved in THF/DMF 4:1 (3 mL), KO$^t$Bu (5 mg, 0.043 mmol) and MeI (15 mg, 1.06 mmol) were added, and the reaction mixture was stirred at RT overnight. Solvents were removed under reduced pressure, and the residue was taken up in EtOAc (7 mL). This was extracted with sat. aq. NaCl (3 mL), sat. aq. $NaHCO_3$ (3 mL), sat. aq. $NH_4Cl$ (3 mL), and finally sat. aq. NaCl (3 mL). The organic layer was dried over $Na_2SO_4$ and evaporated yielding probe **15** (14.5 mg, 88%). UV/vis (PBS buffer): $\lambda_{max}$ abs. 327 nm. $^1$H NMR (300 MHz, $CDCl_3$) $\delta$ 8.39−8.27 (m, 1H), 7.41−7.32 (m, 4H), 7.25−7.20 (m, 1H), 7.07 (d, $J$ = 7.9, 2H), 6.73 (d, $J$ = 8.7, 1H), 4.70−4.49 (m, 1H), 4.02 (s, 3H), 3.80 (s, 2H), 3.03 (d, $J$ = 11.2, 2H), 2.43 (td, $J$ = 12.1, 6.4, 2H), 2.01−1.77 (m, 3H), 1.53 (br, 1H), 1.39−1.25 (m, 2H), 1.00 (d, $J$ = 13.0, 2H). $^{13}$C NMR (100 MHz, $CD_3OD$) $\delta$ 164.1, 141.9, 128.1, 126.8, 126.2, 125.8, 122.4, 122.0, 108.4, 54.8, 48.8, 40.5, 35.3, 32.9, 24.2, 20.5, 15.4. HRMS $m/z$ calcd for $C_{26}H_{28}F_3N_6O$ $[M + H]^+$ 497.2271, found 497.2262.

*1-(Prop-2-yn-1-yl)-N-((1R,3r,5S)-9-(4-(3-(trifluoromethyl)-3H-diazirin-3-yl)benzyl)-9-azabicyclo[3.3.1]nonan-3-yl)-1H-indazole-3-carboxamide (**16**).* Indazole carboxamide **14** (24 mg, 0.05 mmol) was dissolved in DMF (1 mL) under dry conditions, $Cs_2CO_3$ (42.7 mg, 0.131 mmol) was added, and the solution was stirred at RT for 20 min. 3-Bromoprop-1-yne (8.2 mg, 0.068 mmol) was added, and the reaction mixture was stirred at RT for 4 h. Solvents were removed *in vacuo*, sat. aq. $NaHCO_3$ (5 mL) was added, and the mixture was extracted with DCM (3 × 20 mL). The combined organic layers were dried ($Na_2SO_4$)


DOI: 10.1021/acschemneuro.8b00327
ACS Chem. Neurosci. 2019, 10, 438−450

and evaporated to give probe **16** (24.2 mg, 93%). UV/vis (PBS buffer): $\lambda_{max}$ abs. 316 nm. IR: 3309, 2926, 2359, 2343, 1642, 1539, 1343, 1311, 1231, 1181, 1154, 937 $cm^{-1}$. $^1H$ NMR (300 MHz, DMSO-$d_6$) $\delta$ 8.22 (d, $J$ = 8.1, 1H), 8.15 (d, $J$ = 9.1, 1H), 7.81 (d, $J$ = 8.5, 1H), 7.52 (m, 3H), 7.34 (d, $J$ = 7.3, 1H), 7.29 (d, $J$ = 8.6, 2H), 5.58 (d, $J$ = 7.8, 1H), 5.44 (d, $J$ = 2.4, 2H), 4.58−4.42 (m, 1H), 3.89 (s, 2H), 3.02 (d, $J$ = 10.8, 2H), 2.26−2.11 (m, 3H), 1.92 (t, $J$ = 14.1, 2H), 1.80−1.40 (m, 4H), 1.00 (d, $J$ = 15.8, 2H). $^1H$ NMR (300 MHz, $CDCl_3$) $\delta$ 8.36 (d, $J$ = 8.2, 2H), 7.49 (d, $J$ = 8.5, 1H), 7.36−7.41 (m, 3H), 7.25 (m, 1H), 7.07 (d, $J$ = 8.0, 2H), 6.73 (d, $J$ = 8.7, 1H), 5.12 (d, $J$ = 2.5, 2H), 4.67−4.52 (m, 1H), 4.02 (d, $J$ = 7.9, 1H), 3.48−3.34 (m, 1H), 3.03 (d, $J$ = 10.9, 2H), 2.52−2.39 (m, 2H), 2.37 (t, $J$ = 2.5, 1H), 1.94−1.80 (m, 2H), 1.68−1.45 (m, 2H), 1.40−1.28 (m, 2H), 1.03−0.93 (m, 2H). $^{13}C$ NMR (75 MHz, $CDCl_3$) $\delta$ 161.7, 156.7, 142.5, 140.6, 138.5, 128.7, 127.4, 126.5, 123.5, 122.9, 120.4, 109.4, 77.2, 76.5, 74.3, 55.5, 49.3, 41.2, 39.4, 34.0, 33.5, 25.6, 24.9, 14.3. $^{19}F$-NMR (376 MHz, DMSO-$d_6$) $\delta$ −64.6. HRMS $m/z$ calcd for $C_{28}H_{28}F_3N_6O$ $[M + H]^+$ 521.2271, found 521.2267.

**Biology.** Materials, human embryonic kidney (HEK) 293T cell culture maintenance, 5-$HT_3$ receptor expression, 5-$HT_3$ receptor affinity purification and its micelle solubilization, radioligand binding, and binding data analysis were described previously.[32]

**Photo-cross-linking 5-$HT_3$ Receptor with Granisetron Probes.** For all irradiation experiments a UVP 3UV−38 UV Lamp (Upland, CA, USA) was used and set to an irradiation wavelength of 302 nm (lamp power 8 W).

For whole cell lysate experiments, HEK293T cells stably expressing human N-terminal FLAG-tagged 5-$HT_3$A receptor[32] were defrosted (1.8 mL), and 2 mL of PBS buffer (50 mM NaCl, 0.27 mM KCl, 1 mM $Na_2HPO_4$, 0.2 mM $KH_2PO_4$, pH 7.4), 75 $\mu$L of Halt Protease Inhibitor Cocktail (1×, Thermo Fisher Scientific), 5 $\mu$L of Cyanase Nuclease (50 U/$\mu$L, RiboSolutions Inc.), and 5 $\mu$L of $MnSO_4$ (1 M) were added. The cells were homogenized using a Dounce homogenizer and by aspiration with a syringe through a 21G needle and expulsion through a 27G needle. 5-$HT_3$ receptor-containing whole cell lysate (250 $\mu$L) prepared in this way was incubated with either 2.5 $\mu$L of **6** (25 mM in DMSO), 2.5 $\mu$L of **16** (25 mM in DMSO), or 2.5 $\mu$L of **22** (50 mM in DMSO) at RT for 90 min in the dark and then irradiated on ice for 30 min in a 9-well plate. The solutions were transferred back to tubes, and 250 $\mu$L of PBS was added.

To determine concentration dependence of photo-cross-linking with **6**, a solution of purified, micelle-solubilized FLAG-tagged h5-$HT_3$A receptor was adjusted to a concentration of 8.4 $\mu$g/mL using PBS buffer with 0.4 mM $C_{12}E_9$. In a 48-well plate, 5-$HT_3$ receptor−micelle solutions (100 $\mu$L) were mixed each with 1 $\mu$L of different stock solutions of either **6** or **22** in order to obtain final compound concentrations of 2.5 $\mu$M, 250 nM, 25 nM, and 2.5 nM. The solutions were incubated in the dark for 30 min at RT and then irradiated on ice for 30 min. The samples were diluted with 50 $\mu$L of PBS and transferred back from the wells into tubes.

For competition experiments with granisetron, a solution of purified, micelle-solubilized FLAG-tagged h5-$HT_3$A receptor was adjusted to a concentration of 50 $\mu$g/mL using PBS buffer with 0.4 mM $C_{12}E_9$. Using a 48-well plate, 100 $\mu$L of this 5-$HT_3$ receptor−micelle solution was mixed with 0.5 $\mu$L of granisetron (2.5 mM in DMSO) and incubated for 10 min at RT. Subsequently, either 0.5 $\mu$L of **6** (25 mM in DMSO) or 0.5 $\mu$L of **22** (50 mM) was added, and the samples were incubated for further 30 min in the dark at RT. The samples were then irradiated on ice for 20 min, diluted with PBS (50 $\mu$L), and transferred back to tubes.

For live cell irradiation experiments, HEK293T cells stably expressing human N-terminal FLAG-tagged 5-$HT_3$A receptor were grown to approximately 80% density in four T300 plates. The cells were washed with PBS (10 mL/plate), then incubated with PBS (10 mL/plate) for 10 min at 37 °C and detached by repeatedly flushing them off. The cell suspension was cooled on ice, 300 $\mu$L of Halt Protease Inhibitor Cocktail was added, and the suspension was split into two portions to which probes **6** or **22** were added (100 $\mu$L, 0.5 mM in DMSO). The suspensions were incubated for 15 min at RT in the dark and then irradiated in a 6-well plate on ice for 25 min while the cells were gently stirred. The viability of the cells was monitored during irradiation ($t$ = 0, 10, 20, 25 min) by using a cell counter (Countess automated cell counter, Invitrogen), and results are depicted in Figure S2. For each cell suspension portion (with either **6** or **22**), the cells were pelleted by centrifugation (5 min, 500$g$), the supernatant was discarded, and the volume was increased to 3 mL with PBS buffer. More protease inhibitor cocktail was added (75 $\mu$L), and the cells were homogenized first using a 5 mL Dounce homogenizer and then by aspiration with a syringe through a 21G needle and expulsion through a 27G needle. The membranes were collected by centrifugation at 100 000$g$ for 30 min, pellets were resuspended in 5 mL of solubilization buffer (10 mM phosphate buffer, pH 7.4, 0.5 M NaCl, 10 mM imidazole, 2 mM $C_{12}E_9$), and 2.5 $\mu$L of Cyanase (50 U/mL) and 2.5 $\mu$L of $MnSO_4$ (1 mM) were added. The samples were agitated for 1 h at 4 °C and then centrifuged (1 h, 100 000$g$) to remove insoluble components. The supernatant was incubated head-over-tail with 100 $\mu$L of prewashed FLAG beads (FLAG M2 agarose beads, Sigma) for 2 h at 4 °C. The beads were removed by centrifugation (2 min, 500$g$), washed 5 times with PBS buffer containing 0.4 mM $C_{12}E_9$, and incubated with 125 $\mu$L of elution buffer (wash buffer supplemented with 1 mg/mL FLAG peptide). The suspension was centrifuged (2 min, 500$g$) through Micro Bio-Spin columns, giving the eluate.

**Conjugation with Biotin Tag via CuAAC.** Stock solutions of click reagents biotin-$PEG_2$-azide **23** (5 mM in DMSO), TCEP (50 mM in $H_2O$, freshly prepared prior to each experiment), TBTA (1.7 mM in $t$-BuOH/DMSO 4:1), and $CuSO_4 \cdot 5H_2O$ (50 mM in $H_2O$) were prepared and added in this order to a tube containing alkynylated protein sample obtained from photo-cross-linking with either **6**, **16**, or **22**. A ratio of photo-cross-linking probe/biotin azide/TCEP/TBTA/$CuSO_4$ of 1:1000:1000:3000:1000 was normally used, and the tube was vortexed after addition of each click reagent. The mixture was incubated for 2 h at RT on a vertical rotator and subsequently transferred to a Slide-A-Lyzer MINI Dialysis device (Thermo Fisher, 0.5 mL, 20K MWCO). The protein reaction mixture was dialyzed against PBS buffer (13.5 mL, twice for 2 h at RT, then overnight at 4 °C). For biotin pull-down, PBS buffer prewashed (2 × 25 $\mu$L) Dynabeads MyOne Streptavidin M 270 (Life Technologies) were transferred with PBS (50 $\mu$L) to the dialyzed eluate and incubated overnight. The beads were collected by means of magnet, and the supernatant was removed. The streptavidin beads were washed with 1 mL of $C_{12}E_9$ solution (2 mM in PBS), then PBS (3 × 1 mL), and incubated with 80 $\mu$L of LDS loading buffer (containing 2 mM biotin) for 10 min at 95 °C for SDS gel analysis.

**Western Blot.** The protein samples from irradiation and subsequent biotinylation experiments were loaded and run on a SDS-PAGE gel. Protein bands were transferred to a membrane using iBlot Novex Gel Transfer Stacks. Membranes were blocked for 30 min with SeaBlock blocking buffer at RT and then incubated with IRDye 800CW streptavidin (Li-Cor, diluted 1:10000 in SeaBlock buffer with 0.2% SDS) for 30 min. The membranes were washed with TBS-Tween buffer (5 × 5 min), then blocked with TBS-Tween milk (0.1% Tween-20, 5% skim milk powder) for 30 min and incubated with rabbit anti-FLAG (Bethyl Laboratories, diluted 1:2000 in TBS-Tween milk) overnight at 4 °C. Membranes were rinsed with TBS-Tween (5 × 5 min) and then incubated with donkey anti-rabbit IRDye 680 (Li-Cor, diluted 1:10000 in TBS-Tween milk) for 2 h at RT. The membranes were rinsed with TBS-Tween (5 × 5 min), dried, and then imaged using a Li-Cor Odyssey Fluorescent Imaging System.

**Protein Mass Spectrometry.** Protein mixtures from photo-cross-linking experiments were run on a SDS-PAGE gel; the gel was fixed for 10 min with $H_2O$/MeOH/AcOH 5:4:1, washed with $H_2O$ (3 × 5 min), and then stained with Colloidal Coomassie for 2 h. The gel was rinsed with $H_2O$ for 1 h, and protein bands between 50 and 60 kDa cut out under sterile conditions. Gel cubes were washed with 50 mM Tris/HCl, pH 8 (Tris buffer), and Tris buffer/MeCN 50:50 before disulfide reduction with 50 mM DTT (Fluka, Buchs, Switzerland) in Tris buffer for 30 min at 37 °C and subsequent thiol alkylation with 50 mM iodoacetamide (Fluka) in Tris buffer for 30 min at 37 °C in the dark. After washing with Tris buffer and dehydration with MeCN, the gel cubes were soaked with trypsin solution composed of 10 ng/$\mu$L trypsin (Promega) in 20 mM Tris/HCl, pH 8, with 0.01% ProteaseMax


DOI: 10.1021/acschemneuro.8b00327
ACS Chem. Neurosci. 2019, 10, 438−450

(Promega) for 30 min on ice. Gel cubes were subsequently covered with 5−10 mL of 20 mM Tris/HCl before digestion for 1 h at 50 °C. For digestions with Proteinase K (1 ng/μL and 10 ng/μL, Promega), AspN (10 ng/μL, Roche), and LysC/trypsin mix (10 ng/μL, Promega), ProteaseMax was not included in the digestion buffer, and incubations were 30 min on ice and 30 min at 37 °C, 6 h at 37 °C, and 16 h at RT, respectively. The supernatant liquid was combined with a single gel extract performed with 20 mL of 20% (v/v) formic acid (Merck) in polypropylene HPLC vials, and 5 μL was analyzed by LC-MS/MS (PROXEON coupled to a QExactive mass spectrometer, Thermo-Fisher Scientific).

Peptides were trapped on an μPrecolumn C18 PepMap100 (5 μm, 100 Å, 300 μm × 5 mm, ThermoFisher Scientific, Reinach, Switzerland) and separated by backflush on a C18 column (3 μm, 100 Å, 75 μm × 15 cm, Nikkyo Technos, Tokyo, Japan) by applying a 30 min gradient of 5% to 40% MeCN in $H_2O$, 0.1% formic acid, at a flow rate of 300 nL/min. Peptides of $m/z$ 360−1400 were detected on the QExactive with resolution set at 70 000 with an automatic gain control (AGC) target of $1 \times 10^6$, and maximum ion injection time of 50 ms. A top ten data dependent method for precursor ion fragmentation was applied with the following settings: resolution 17 500, AGC of $1 \times 10^5$, maximum ion time of 110 ms, mass window 2 $m/z$, collision energy 27, underfill ratio 1%, charge exclusion of unassigned and 1+ ions, and peptide match on.

Fragment spectra information was extracted into mgf file format using ProteomeDiscoverer v1.3 software (ThermoFisher Scientific). Fragment spectra interpretation was performed with ProteomeDiscoverer v1.3 against human database, using fixed modifications of carbamidomethylation on cysteine, and variable modifications of oxidation on methionine, acetylation on protein N-terminus, and photo-cross-linking probes on certain amino acids. Protein identifications were considered with at least two unique peptides identified at a 1% FDR on the level of peptide spectrum matches. Fragment peptide sequences were identified with the Sequest HT (v1.3) search engine implemented in the ProteomeDiscoverer software.

**Molecular Modeling.** Homologous AChBP chimera bound with granisetron (PDB ID 2YME) was used as a protein template for the docking. This chimera, termed 5HTBP, has substitutions in the orthosteric binding site that mimic the 5-$HT_3$ receptor.[14] The ligands **4** and **10** were constructed ab initio in Chem3D Pro v14.0 (PerkinElmer, Waltham, MA), based on the crystal structure of granisetron extracted from the Cambridge Structural Database (CSD ID: KUQDAC), and energy-minimized using the included MM2 force field. A library of 200 conformers was generated for each ligand using OMEGA v2.5 (OpenEye Scientific Software, Santa Fe, NM). To generate a docking template from the 2YME crystal structure, FRED RECEPTOR v2.2.5 (OpenEye Scientific Software) was utilized, whereby the ligand binding site was defined as a box of $V = 5143$ Å$^3$ around the bound granisetron. The constructed ligands were docked into this binding site template, in order to predict their binding poses, using FRED v2.1 (OpenEye Scientific Software) that utilizes an exhaustive process to position and score all conformers of a ligand at all possible positions within the defined binding site. For each ligand, ten docking poses were generated and ranked using the inbuilt Chemgauss3 scoring function. The proposed binding poses were visualized with PyMOL v1.7 (Schrödinger LLC, Portland, OR).

## ■ ASSOCIATED CONTENT

### Supporting Information

The Supporting Information is available free of charge on the ACS Publications website at DOI: 10.1021/acschemneuro.8b00327.

Chemistry general procedures and synthesis of photo-cross-linking moieties, whole cell lysate photo-cross-linking, MS sequence coverage of 5-$HT_3$A receptor with different digestion protocols, MS/MS of oxidized loop C peptide fragments photo-cross-linked with **4** and **10**, docking of granisetron into 5HTBP, alternative docking poses for **4** and **10**, and copies of NMR spectra of final compounds (PDF)

## ■ AUTHOR INFORMATION


### Corresponding Author

*M.L. Phone: +41 31 631 3311. Fax: +41 31 631 4272. E-mail: martin.lochner@ibmm.unibe.ch.

### ORCID

Martin Lochner: 0000-0003-4930-1886

### Present Addresses

[▽]M.D.R: United Kingdom Dementia Research Institute at King's College London, Institute of Psychiatry, Psychology and Neuroscience, King's College London, London SE5 9NU, U.K. [⊥]S.K.V.V: Center for Drug Design, University of Minnesota, Minneapolis, MN 55455, USA.


### Author Contributions

T.J. performed the chemical synthesis, protein purification, and photo-cross-linking experiments. Mi.L. analyzed the mass spectrometry data and wrote the manuscript. M.D.R. established the protein purification and supported T.J. with the photo-cross-linking experiments. A.J.T. measured binding affinity of probes and wrote the manuscript. S.B.L. performed protein mass spectrometry analysis and analyzed mass spectrometry data. M.H. supervised protein mass spectrometry and discussed experimental data. M.L. planned and coordinated the study, designed and supervised chemical synthesis and photo-cross-linking experiments, and wrote the manuscript.


### Funding

This study was supported by the Swiss National Science Foundation (SNSF professorship PP00P2_123536 and PP00P2_146321 to M.L.) and the British Heart Foundation (PG/13/39/30293 to A.J.T). M.D.R. was supported by the HOLCIM Stiftung zur Förderung der wissenschaftlichen Fortbildung.


### Notes

The authors declare no competing financial interest.

## ■ ACKNOWLEDGMENTS


We acknowledge the analytical services from the Department of Chemistry and Biochemistry, University of Bern, for measuring NMR and MS spectra of synthetic intermediates and final compounds.


## ■ ABBREVIATIONS

AChBP, acetylcholine binding protein; $C_{12}E_9$, nonaethylene glycol monododecyl ether; CuAAC, Cu(I)-catalyzed alkyne−azide cycloaddition; DCM, dichloromethane; ECD, extracellular domain; EM, electron microscopy; GABA, γ-aminobutyric acid (receptor); HATU, 1-[bis(dimethylamino)methylene]-1*H*-1,2,3-triazolo[4,5-*b*]pyridinium 3-oxide hexafluorophosphate; IBS, irritable bowel syndrome; ICD, intracellular domain; nACh, nicotinic acetylcholine (receptor); PET, positron emission tomography; P-PALM, post-photoaffinity modification; SAR, structure−activity relationship; SSRIs, selective serotonin reuptake inhibitors; TBAF, tetra-*n*-butylammonium fluoride; TBS, *tert*-butyldimethylsilyl; TBTA, tris((1-benzyl-1*H*-1,2,3-triazol-4-yl)methyl)amine; TCEP, tris(2-carboxyethyl)phosphine; THF, tetrahydrofuran; TMD, transmembrane domain

## ■ REFERENCES


(1) Hannon, J., and Hoyer, D. (2008) Molecular biology of 5-HT receptors. *Behav. Brain Res. 195*, 198−213.




DOI: 10.1021/acschemneuro.8b00327
*ACS Chem. Neurosci.* 2019, 10, 438−450

(2) Nichols, D. E., and Nichols, C. D. (2008) Serotonin receptors. *Chem. Rev. 108*, 1614−1641.
(3) Thompson, A. J. (2013) Recent developments in 5-$HT_3$ receptor pharmacology. *Trends Pharmacol. Sci. 34*, 100−109.
(4) Lummis, S. C. R. (2012) 5-$HT_3$ receptors. *J. Biol. Chem. 287*, 40239−40245.
(5) Moore, N. A., Sargent, B. J., Manning, D. D., and Guzzo, P. R. (2013) Partial agonism of 5-$HT_3$ receptors: a novel approach to the symptomatic treatment of IBS-D. *ACS Chem. Neurosci. 4*, 43−47.
(6) Walstab, J., Rappold, G., and Niesler, B. (2010) 5-$HT_3$ receptors: role in disease and target of drugs. *Pharmacol. Ther. 128*, 146−169.
(7) Machu, T. K. (2011) Therapeutics of 5-$HT_3$ receptor antagonists: current uses and future directions. *Pharmacol. Ther. 130*, 338−347.
(8) Bétry, C., Etiévant, A., Oosterhof, C., Ebert, B., Sanchez, C., and Haddjeri, N. (2011) Role of 5-$HT_3$ receptors in the antidepressant response. *Pharmaceuticals 4*, 603.
(9) Joshi, P. R., Suryanarayanan, A., Hazai, E., Schulte, M. K., Maksay, G., and Bikadi, Z. (2006) Interactions of granisetron with an agonist-Free 5-$HT_{3A}$ receptor model. *Biochemistry 45*, 1099−1105.
(10) Nyce, H. L., Stober, S. T., Abrams, C. F., and White, M. M. (2010) Mapping spatial relationships between residues in the ligand-binding domain of the 5-$HT_3$ receptor using a molecular ruler. *Biophys. J. 98*, 1847−1855.
(11) Thompson, A. J., Price, K. L., Reeves, D. C., Ling Chan, S., Chau, P.-L., and Lummis, S. C. R. (2005) Locating an antagonist in the 5-$HT_3$ receptor binding site using modeling and radioligand binding. *J. Biol. Chem. 280*, 20476−20482.
(12) Hassaine, G., Deluz, C., Grasso, L., Wyss, R., Tol, M. B., Hovius, R., Graff, A., Stahlberg, H., Tomizaki, T., Desmyter, A., Moreau, C., Li, X.-D., Poitevin, F., Vogel, H., and Nury, H. (2014) X-ray structure of the mouse serotonin 5-$HT_3$ receptor. *Nature 512*, 276−281.
(13) Basak, S., Gicheru, Y., Samanta, A., Molugu, S. K., Huang, W., Fuente, M. l. d., Hughes, T., Taylor, D. J., Nieman, M. T., Moiseenkova-Bell, V., and Chakrapani, S. (2018) Cryo-EM structure of 5-$HT_{3A}$ receptor in its resting conformation. *Nat. Commun. 9*, 514.
(14) Kesters, D., Thompson, A. J., Brams, M., van Elk, R., Spurny, R., Geitmann, M., Villalgordo, J. M., Guskov, A., Helena Danielson, U., Lummis, S. C. R., Smit, A. B., and Ulens, C. (2013) Structural basis of ligand recognition in 5-$HT_3$ receptors. *EMBO Rep. 14*, 49−56.
(15) Price, K. L., Lillestol, R. K., Ulens, C., and Lummis, S. C. R. (2016) Palonosetron−5-$HT_3$ receptor interactions as shown by a binding protein cocrystal structure. *ACS Chem. Neurosci. 7*, 1641−1646.
(16) Ruepp, M.-D., Wei, H., Leuenberger, M., Lochner, M., and Thompson, A. J. (2017) The binding orientations of structurally-related ligands can differ; A cautionary note. *Neuropharmacology 119*, 48−61.
(17) Hamouda, A. K., Sanghvi, M., Chiara, D. C., Cohen, J. B., and Blanton, M. P. (2007) Indentifying the lipid-protein interface of the $\alpha 4\beta 2$ neuronal nicotinic acetylcholine receptor: Hydrophobic photolabeling studies with 3-(trifluoromethyl)-3-(*m*-[$^{125}$I]iodophenyl)-diazirine. *Biochemistry 46*, 13837−13846.
(18) Hamouda, A., Jayakar, S., Chiara, D., and Cohen, J. (2014) Photoaffinity labeling of nicotinic receptors: Diversity of drug binding sites! *J. Mol. Neurosci. 53*, 480−486.
(19) Nirthanan, S., Ziebell, M. R., Chiara, D. C., Hong, F., and Cohen, J. B. (2005) Photolabeling the *Torpedo* nicotinic acetylcholine receptor with 4-azido-2,3,5,6-tetrafluorobenzoylcholine, a partial agonist. *Biochemistry 44*, 13447−13456.
(20) Husain, S. S., Stewart, D., Desai, R., Hamouda, A. K., Li, S. G.-D., Kelly, E., Dostalova, Z., Zhou, X., Cotten, J. F., Raines, D. E., Olsen, R. W., Cohen, J. B., Forman, S. A., and Miller, K. W. (2010) *p*-Trifluoromethyldiazirinyl-etomidate: A potent photoreactive general anesthetic derivative of etomidate that is selective for ligand-gated ion channels. *J. Med. Chem. 53*, 6432−6444.
(21) Matsuda, K., Ihara, M., Nishimura, K., Sattelle, D. B., and Komai, K. (2001) Insecticidal and neural activities of candidate photoaffinity probes for neonicotinoid binding sites. *Biosci., Biotechnol., Biochem. 65*, 1534−1541.
(22) Mortensen, M., Iqbal, F., Pandurangan, A. P., Hannan, S., Huckvale, R., Topf, M., Baker, J. R., and Smart, T. G. (2014) Photo-antagonism of the $GABA_A$ receptor. *Nat. Commun. 5*, 4454.
(23) Tomizawa, M., Maltby, D., Medzihradszky, K. F., Zhang, N., Durkin, K. A., Presley, J., Talley, T. T., Taylor, P., Burlingame, A. L., and Casida, J. E. (2007) Defining nicotinic agonist binding surface through photoaffinity labelling. *Biochemistry 46*, 8798−8806.
(24) Yip, G. M. S., Chen, Z.-W., Edge, C. J., Smith, E. H., Dickinson, R., Hohenester, E., Townsend, R. R., Fuchs, K., Sieghart, W., Evers, A. S., and Franks, N. P. (2013) A propofol binding site on mammalian $GABA_A$ receptors identified by photolabeling. *Nat. Chem. Biol. 9*, 715−720.
(25) Tanaka, Y., Bond, M. R., and Kohler, J. J. (2008) Photo-crosslinkers illuminate interactions in living cells. *Mol. BioSyst. 4*, 473−480.
(26) Dubinsky, L., Krom, B. P., and Meijler, M. M. (2012) Diazirine based photoaffinity labeling. *Bioorg. Med. Chem. 20*, 554−570.
(27) Nakata, E., Nagase, T., Shinkai, S., and Hamachi, I. (2004) Coupling a natural receptor protein with an artificial receptor to afford a semisynthetic fluorescent biosensor. *J. Am. Chem. Soc. 126*, 490−495.
(28) Kiyonaka, S., Kato, K., Nishida, M., Mio, K., Numaga, T., Sawaguchi, Y., Yoshida, T., Wakamori, M., Mori, E., Numata, T., Ishii, M., Takemoto, H., Ojiida, A., Watanabe, K., Uemura, A., Kurose, H., Morii, T., Kobayashi, T., Sato, Y., Sato, C., Hamachi, I., and Mori, Y. (2009) Selective and direct inhibition of TRPC3 channels underlies biological activities of a pyrazole compound. *Proc. Natl. Acad. Sci. U. S. A. 106*, 5400−5405.
(29) Sanghvi, M., Hamouda, A. K., Davis, M. I., Morton, R. A., Srivastava, S., Pandhare, A., Duddempudi, P. K., Machu, T. K., Lovinger, D. M., Cohen, J. B., and Blanton, M. P. (2009) Hydrophobic photolabeling studies identify the lipid−protein interface of the 5-$HT_3$A receptor. *Biochemistry 48*, 9278−9286.
(30) Lummis, S. C. R., and Baker, J. (1997) Radioligand binding and photoaffinity labelling studies show a direct interaction of phenothiazines at 5-$HT_3$ receptors. *Neuropharmacology 36*, 665−670.
(31) Simonin, J., Vernekar, S. K. V., Thompson, A. J., Hothersall, J. D., Connolly, C. N., Lummis, S. C. R., and Lochner, M. (2012) High-affinity fluorescent ligands for the 5-$HT_3$ receptor. *Bioorg. Med. Chem. Lett. 22*, 1151−1155.
(32) Jack, T., Simonin, J., Ruepp, M. D., Thompson, A. J., Gertsch, J., and Lochner, M. (2015) Characterizing new fluorescent tools for studying 5-$HT_3$ receptor pharmacology. *Neuropharmacology 90*, 63−73.
(33) Lochner, M., and Thompson, A. J. (2015) A review of fluorescent ligands for studying 5-$HT_3$ receptors. *Neuropharmacology 98*, 31−40.
(34) Mu, L., Müller Herde, A., Rüefli, P. M., Sladojevich, F., Milicevic Sephton, S., Krämer, S. D., Thompson, A. J., Schibli, R., Ametamey, S. M., and Lochner, M. (2016) Synthesis and pharmacological evaluation of [$^{11}$C]granisetron and [$^{18}$F]fluoropalonosetron as PET probes for 5-$HT_3$ receptor imaging. *ACS Chem. Neurosci. 7*, 1552−1564.
(35) Vernekar, S. K. V., Hallaq, H. Y., Clarkson, G., Thompson, A. J., Silvestri, L., Lummis, S. C. R., and Lochner, M. (2010) Toward biophysical probes for the 5-$HT_3$ receptor: structure−activity relationship study of granisetron derivatives. *J. Med. Chem. 53*, 2324−2328.
(36) Patricelli, M. P., and Cravatt, B. F. (2001) Characterization and manipulation of the acyl chain selectivity of fatty acid amide hydrolase. *Biochemistry 40*, 6107−6115.
(37) Strømgaard, K., Saito, D. R., Shindou, H., Ishii, S., Shimizu, T., and Nakanishi, K. (2002) Ginkgolide derivatives for photolabeling studies: preparation and pharmacological evaluation. *J. Med. Chem. 45*, 4038−4046.
(38) Hatanaka, Y., Nakayama, H., and Kanaoka, Y. (1993) An improved synthesis of 4-[3-(trifluoromethyl)-3*H*-diazirin-3-yl]benzoic acid for photoaffinity labeling. *Heterocycles 35*, 997−1004.
(39) Jack, T., Ruepp, M.-D., Thompson, A. J., Mühlemann, O., and Lochner, M. (2014) Synthesis and characterization of photoaffinity probes that target the 5-$HT_3$ receptor. *Chimia 68*, 239−242.
(40) Yang, Z., and Manning, D. D. (2008) 2-Alkylbenzoxazole carboxamides as 5-$HT_3$ modulators. U.S. Patent US2008/0214601A1.


DOI: 10.1021/acschemneuro.8b00327
*ACS Chem. Neurosci.* 2019, 10, 438−450

(41) Shih, L. B., and Bayley, H. (1985) A carbene-yielding amino acid for incorporation into peptide photoaffinity reagents. *Anal. Biochem. 144*, 132−141.
(42) Smith, D. P., Anderson, J., Plante, J., Ashcroft, A. E., Radford, S. E., Wilson, A. J., and Parker, M. J. (2008) Trifluoromethyldiazirine: an effective photo-induced cross-linking probe for exploring amyloid formation. *Chem. Commun.*, 5728−5730.
(43) Bandyopadhyay, S., and Bong, D. (2011) Synthesis of trifunctional phosphatidylserine probes for identification of lipid-binding proteins. *Eur. J. Org. Chem. 2011*, 751−758.
(44) van Scherpenzeel, M., Moret, E. E., Ballell, L., Liskamp, R. M. J., Nilsson, U. J., Leffler, H., and Pieters, R. J. (2009) Synthesis and evaluation of new thiodigalactoside-based chemical probes to label Galectin-3. *ChemBioChem 10*, 1724−1733.
(45) Hope, A. G., Peters, J. A., Brown, A. M., Lambert, J. J., and Blackburn, T. P. (1996) Characterization of a human 5-hydroxytryptamine$_3$ receptor type A (h5-HT3R-A$_S$) subunit stably expressed in HEK 293 cells. *Br. J. Pharmacol. 118*, 1237−1245.
(46) Beene, D. L., Brandt, G. S., Zhong, W., Zacharias, N. M., Lester, H. A., and Dougherty, D. A. (2002) Cation-$\pi$ interactions in ligand recognition by serotonergic (5-HT$_{3A}$) and nicotinic acetylcholine receptors: The anomalous binding properties of nicotine. *Biochemistry 41*, 10262−10269.
(47) Duffy, N. H., Lester, H. A., and Dougherty, D. A. (2012) Ondansetron and granisetron binding orientation in the 5-HT$_3$ receptor determined by unnatural amino acid mutagenesis. *ACS Chem. Biol. 7*, 1738−1745.
(48) Thompson, A. J., Lester, H. A., and Lummis, S. C. R. (2010) The structural basis of function in Cys-loop receptors. *Q. Rev. Biophys. 43*, 449−499.


DOI: 10.1021/acschemneuro.8b00327
*ACS Chem. Neurosci.* 2019, 10, 438−450